GEOLOGICAL AND GEOCHEMICAL EVIDENCE FOR A LATE CRETACEOUS CONTINENTAL ARC IN THE CENTRAL PONTIDES, NORTHERN TURKEY

Alessandro Ellero°,✉, Giuseppe Ottria°, Kaan Sayit*, Rita Catanzariti°, Chiara Frassi, M. Cemal Göncüoğlu*, Michele Marroni**,° and Luca Pandolfi**,°**

° *CNR-Istituto di Geoscienze e Georisorse, Pisa, Italy.*
* *Department of Geological Engineering, Middle East Technical University, Ankara, Turkey.*
** *Dipartimento di Scienze della Terra, Università di Pisa, Italy.*
✉ *Corresponding author: e-mail: ellero@igg.cnr.it*

Keywords: *continental arc magmatism, volcaniclastic succession, geochemistry, structural geology, Late Cretaceous. Central Pontides, Turkey.*

ABSTRACT

In the Central Pontides (Northern Turkey), south of Tosya, a tectonic unit consisting of not-metamorphic volcanic rocks and overlying sedimentary succession is exposed inside a fault-bounded elongated block. It is restrained within a wide shear zone, where the Intra-Pontide suture zone, the Sakarya terrane and the Izmir-Ankara-Erzincan suture zone are juxtaposed as result of strike-slip activity of the North Anatolian shear zone. The volcanic rocks are mainly basalts and basaltic andesites (with their pyroclastic equivalents) associated with a volcaniclastic formation made up of breccias and sandstones that are stratigraphically overlain by a Marly-calcareous turbidite formation. The calcareous nannofossil biostratigraphy points to a late Santonian-middle Campanian age (CC17-CC21 Zones) for the sedimentary succession. The geochemistry of the volcanic rocks reveals an active continental margin setting as evidenced by the enrichment in Th and LREE over HFSE, and the Nb-enriched nature of these lavas relative to N-MORB. As highlighted by the performed arenite petrography, the occurrence of continent-derived clastics in the sedimentary succession supports the hypothesis of a continental arc-derived volcanic succession. Alternative geodynamic reconstructions are proposed, where this tectonic unit could represent a slice derived from the northern continental margin of the Intra-Pontide or Izmir-Ankara-Erzincan oceanic basins.

INTRODUCTION

The tectonic setting of Turkey results from the progressive accretion of Gondwana-derived fragments to the Eurasian plate as a consequence of the closure of several Paleo- and Neo-Tethyan oceanic basins. The result is an assemblage of continental terranes bounded by ophiolite-bearing suture zones whose ages range from Late Neoproterozoic to Cretaceous (Göncüoğlu et al., 1997 and quoted references).

The Intra-Pontide suture zone (Göncüoğlu et al., 2000) is the northernmost ophiolitic suture zone cropping out in Turkey. It extends from the Biga Peninsula, in the west, to Kargi Massif, in the east (Şengör and Yilmaz, 1981; Robertson and Ustaömer, 2004, Göncüoğlu et al., 2006) (Fig. 1a). The Intra-Pontide suture zone testifies the presence of an oceanic basin, the Intra-Pontide oceanic basin, opened in the Middle Triassic time between two continental terranes today represented by the Istanbul-Zonguldak terrane, to the north, and the Sakarya terrane, to the south (Şengör and Yılmaz, 1981; Göncüoğlu et al., 1987; 2008; Yılmaz, 1990; Göncüoğlu and Erendil, 1990; Robertson et al., 1991; Yılmaz et al., 1995; 1997; Okay and Tüysüz, 1999; Elmas and Yiğitbaş, 2001; Robertson and Ustaömer, 2004; Göncüoğlu et al., 2008; Akbayram et al., 2012). Since the Middle Jurassic, the convergence between Gondwanan and Laurasian continental plates originated the development of a subduction zone leading to progressive closure of the Intra-Pontide oceanic basin. The complete closure of the Intra-Pontide oceanic basin and the collision between Istanbul-Zonguldak and Sakarya terranes occurred in the Late Paleocene (Catanzariti et al., 2013). As a consequence, the units derived from both the Intra-Pontide oceanic basin and its continental margins were imbricated trough top-to-the-S low-angle thrusts in a tectonic stack (Şengör and Yılmaz, 1981; Okay et al., 1996; Okay, 2000). The resulting architecture shows the Istanbul-Zonguldak terrane thrusts on both Intra-Pontide suture zone and Sakarya terrane.

The Istanbul-Zonguldak terrane, north of the Intra-Pontide suture zone, includes a Neoproterozoic basement unconformably overlain by an Ordovician to Carboniferous sedimentary succession, only weakly deformed during the Variscan orogeny (e.g., Görür et al., 1997). This succession is unconformably overlain by a thick sequence of Late Permian-Late Jurassic deposits, in turn covered by Late Cretaceous-Paleocene turbidite deposits (Akveren Flysch) where andesitic volcanic flows have been found (e.g., Aydın et al., 1986).

The Sakarya terrane, south of the Intra-Pontide suture zone, comprises a Variscan arc and its Permo-Triassic cover, tectonically imbricated with remnants of the Late Paleozoic-Triassic Paleo-Tethys (Karakaya Complex *sensu* Okay and Göncüoğlu, 2004; Sayit and Göncüoğlu, 2013). The overstep sequence of the Sakarya terrane comprises Jurassic-Late Cretaceous platform to slope sediments, respectively, followed by foreland deposits represented by Late Cretaceous-Early Paleogene turbidites.

South of the Sakarya terrane, the Izmir-Ankara-Erzincan suture zone preserves the remnants of the main Neo-Tethyan oceanic branch, of which the Tauride-Anatolide block represents the southern continental margin. In northern Central Anatolia the Izmir-Ankara-Erzincan suture zone is represented by the Ankara Mélange (Rojay, 2013; Bortolotti et al., 2013) consisting of an imbrication of

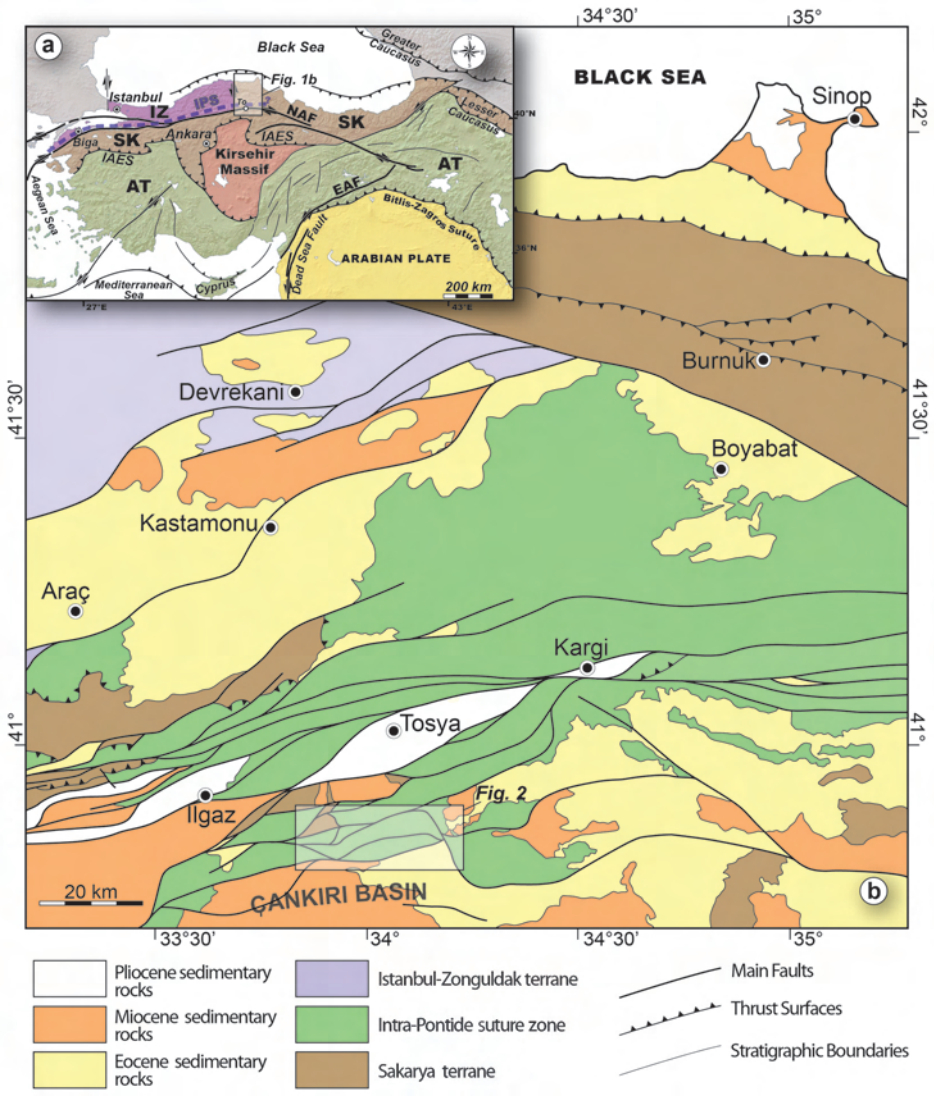

Fig. 1 - a) Tectonic map of Turkey and b) schematic geological map of the Central Pontides. IZT Istanbul-Zonguldak terrane, SKT Sakarya terrane, AT Anatolide-Tauride terrane, NASZ North Anatolian shear zone, EAF East Anatolian fault, IPS Intra-Pontide suture zone.

ophiolites, mélanges and piggy-back deposits of Late Cretaceous age.

In northern Turkey (Figs. 1 and 2), the overall architecture, characterized by two juxtaposed ophiolitic suture zones, has been strongly dismembered by the North Anatolian shear zone (NASZ of Şengör et al., 2005), one of the most important strike-slip continental crustal-scale fault systems in the world. The North Anatolian shear zone corresponds to a complex deformation zone (Fig. 1a) where the strain is partitioned in a system of faults, folds and thrusts (Ellero et al., 2015) leading to high-angle faults bounding ~ E-W elongated blocks and pull-apart basins.

In order to provide valuable insights for deciphering the geodynamic evolution of both the oceanic basins and their margins, we conducted detailed lithostratigraphic, paleontological, petrographic, geochemical and structural investigations in one of these blocks, located 30 km south of Tosya (Fig. 1b). The block consists of an not-metamorphic stratigraphic succession constituted by volcanic rocks and a sedimentary cover. The obtained results, compared with those available in literature for the neighbouring areas, are used to reconstruct the geodynamic history of the Central Pontides and interpreted to constrain the kinematics of the North Anatolian shear zone.

GEOLOGICAL SETTING

In the area between Araç and Tosya (Central Pontides, Northern Turkey), the Intra-Pontide suture zone consists of different tectonic units (Fig. 2), including the Ayli Dağ Ophiolite Unit (Göncüoğlu et al., 2012), the Arkot Dağ Mélange (Göncüoğlu et al., 2014) and four metamorphic units (Sayit et al., 2015) described as Central Pontide Structural Complex by Tekin et al. (2012), corresponding to Central Pontide Supercomplex of Okay et al. (2013).

The Ayli Dağ Ophiolite Unit is a back-arc basin-type ophiolite sequence, including 2- to 3-km-thick hazburgitic peridotites topped by a 500- to 600-m-thick layered gabbro sequence, overlain, in turn by a sheeted dyke complex that shows a transition to 700-1000-m-thick basaltic pillow-lava flows and pillow-breccias. The radiolarian cherts sampled from the top of the pillow lavas yielded radiolarian assemblages of the middle Bathonian to early Callovian age (Göncüoğlu et al., 2012).

The Arkot Dağ Mélange (*i.e.* Kirazbaşı Complex of Aygül et al., 2015a) is a late Santonian chaotic sedimentary deposit where slide-blocks of different sizes and lithologies are enclosed in a sedimentary matrix consisting of shales, coarse-grained arenites, pebbly mudstones and pebbly sand-

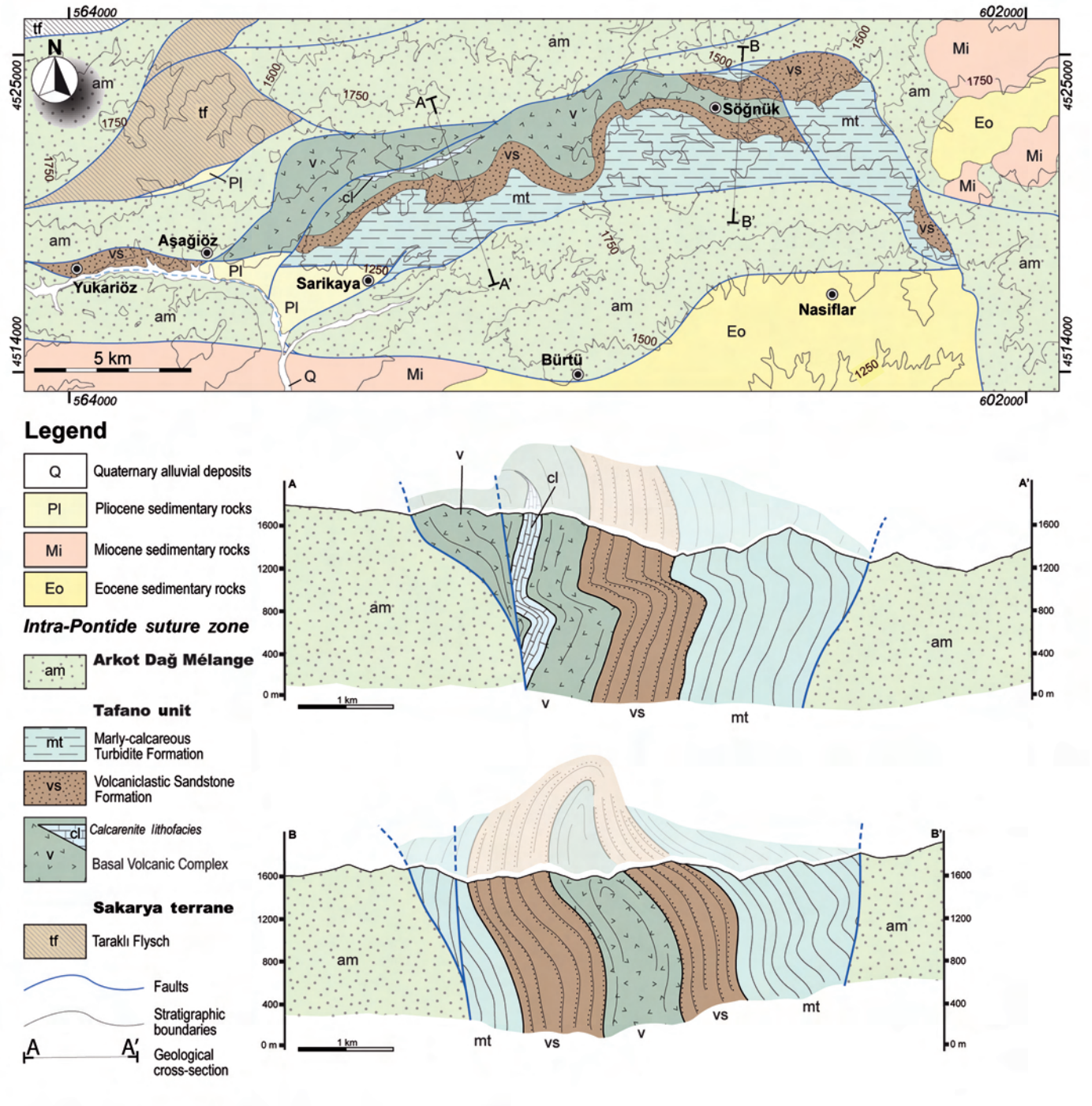

Fig. 2 - Geological sketch map of the study area and geological cross-sections. See Fig. 1b for map location.

stones (Göncüoğlu et al., 2014). The slide-blocks, generally huge, are represented by: (i) metamorphic rocks (mainly micaschists and gneisses), (ii) ophiolites (peridotites, gabbros, basalts and cherts), (iii) sedimentary rocks (cherts, neritic and pelagic limestones, marly-limestones and ophiolite-bearing turbidites). The geochemistry of the basalts shows affinities ranging from Normal-Mid Ocean Ridge Basalts (N-MORB) and Island Arc Tholeiites (IAT) to Back-Arc Basin Basalts (BABB)-type magmas (Göncüoğlu et al. 2008; 2014; Sayit et al., 2015).

The Central Pontide Structural Complex includes four metamorphic units deformed during the closure of the Intra-Pontide oceanic basin in Late Jurassic-Early Cretaceous time span. These units have been deformed and metamorphosed under P/T conditions ranging from very low-grade to blueschist, amphibolite and eclogite-facies (Okay et al., 2006; 2013; Marroni et al., 2014; Aygül et al., 2015a).

In the Central Pontides, the Sakarya terrane is mainly made of Middle Jurassic to Early Cretaceous neritic carbonates and Albian-Cenomanian pelagic limestones showing a transition to Late Cretaceous to Paleocene turbidite deposits (Taraklı Flysch). The Taraklı Flysch is characterized in its uppermost part by carbonate and ophiolite slide-blocks derived from both Istanbul-Zonguldak terrane and

Intra-Pontide suture zone (Catanzariti et al., 2013).

The relationships among these tectonic units are sealed by the late Paleocene sedimentary deposits of the Safranbolu - Karabük Basin (Örzen-Erdem et al., 2005), which is formed above a huge imbricated stack of tectonic units of the Intra-Pontide suture zone. However, this package has been strongly reworked by the North Anatolian shear zone activity since the late Miocene or possibly earlier (Ellero et al., 2015). The shear zone is characterized by the development of several pull-apart basins along the strand of the fault zone, which are used for dating the North Anatolian shear zone activity (Şengör et al., 2005).

One of these, the Tosya Basin, is delimited by NE-SW striking faults and includes late Miocene-Olocene deposits (Barka, 1992; Andrieux et al., 1995; Dhont et al., 1998). South of the Tosya Basin, the pre-Miocene substrate shows a complex setting consisting of a braided pattern of anastomosing faults that bound elongated km-size blocks (Fig. 1b), most derived from Intra-Pontide suture zone and Sakarya terrane. The blocks derived from Intra-Pontide suture zone consist of Arkot Dağ Mélange, those from the Sakarya terrane are represented by Taraklı Flysch (Fig. 2).

In addition, two blocks are characterized by volcanic rocks associated with a sedimentary succession. The first block comprises low-grade metamorphic assemblages of an Early Cretaceous arc and its Late Cretaceous pelagic cover (Kösedağı Unit of Berber et al., 2014, corresponding to Kösdağ paleo-arc of Aygül et al., 2015b). The second block, object of this study, is characterized by a not-metamorphic succession made up of basalt-basaltic andesite topped by a sedimentary cover. We first describe it as a distinct tectonic unit named "Tafano unit" without reference to any location in order to avoid misunderstandings with the names from the previous geological literature. Regionally, the Tafano unit can be roughly correlated with the Campanian-Maastrichtian Yaylacayı and Yapraklı Formations (Tüysüz et al., 1995; Rice et al., 2006). Those formations as well as the Kösdağ paleo-arc are classically ascribed to an intra-oceanic arc setting within the Izmir-Ankara-Erzincan suture zone (Tüysüz et al., 1995; Rice et al., 2006; Aygül et al., 2015a and 2015b). However, as discussed later, we cannot exclude that these units might belong to Intra-Pontide suture zone, as indeed shown in Fig. 1b.

THE TAFANO UNIT

The study area corresponds to the E-W trending strip south of Tosya, including part of the mountain belt between the Tosya Basin, to the north, and the northernmost boundary of the Eocene-Miocene Çankırı Basin, to the south (Fig. 1b).

The Tafano unit is completely bounded by NE-SW trending high-angle faults, separating this unit from the Arkot Dağ Mélange (Fig. 2). The Tafano unit can be subdivided into three formations: (i) Basal Volcanic Complex, (ii) Volcaniclastic Sandstone Formation and (iii) Marly-calcareous Turbidite Formation. The boundaries between these three formations are stratigraphic and their relationships can be observed in the field.

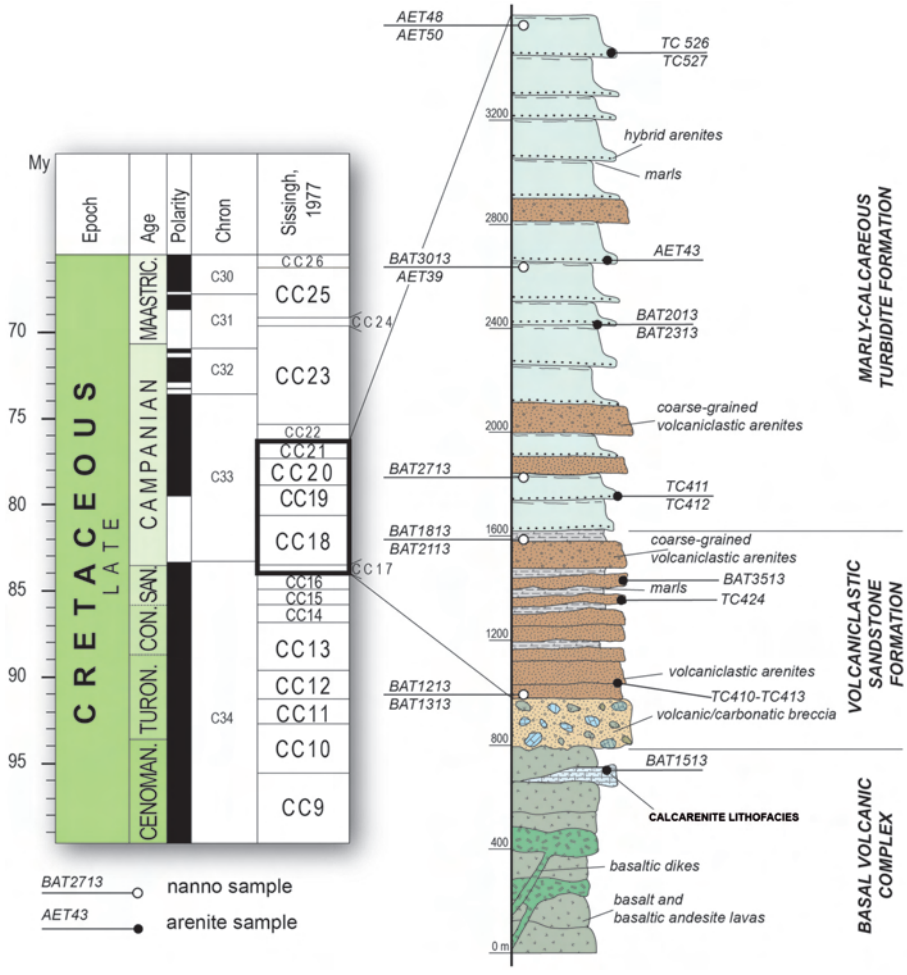

Fig. 3 - Stratigraphic log of the Tafano unit succession with adopted bio-chronostratigraphic scheme. Time scale after Gradstein et al. (2004). Location of samples for nannofossil analyses and arenitic and ruditic samples with respect to stratigraphy is also shown.

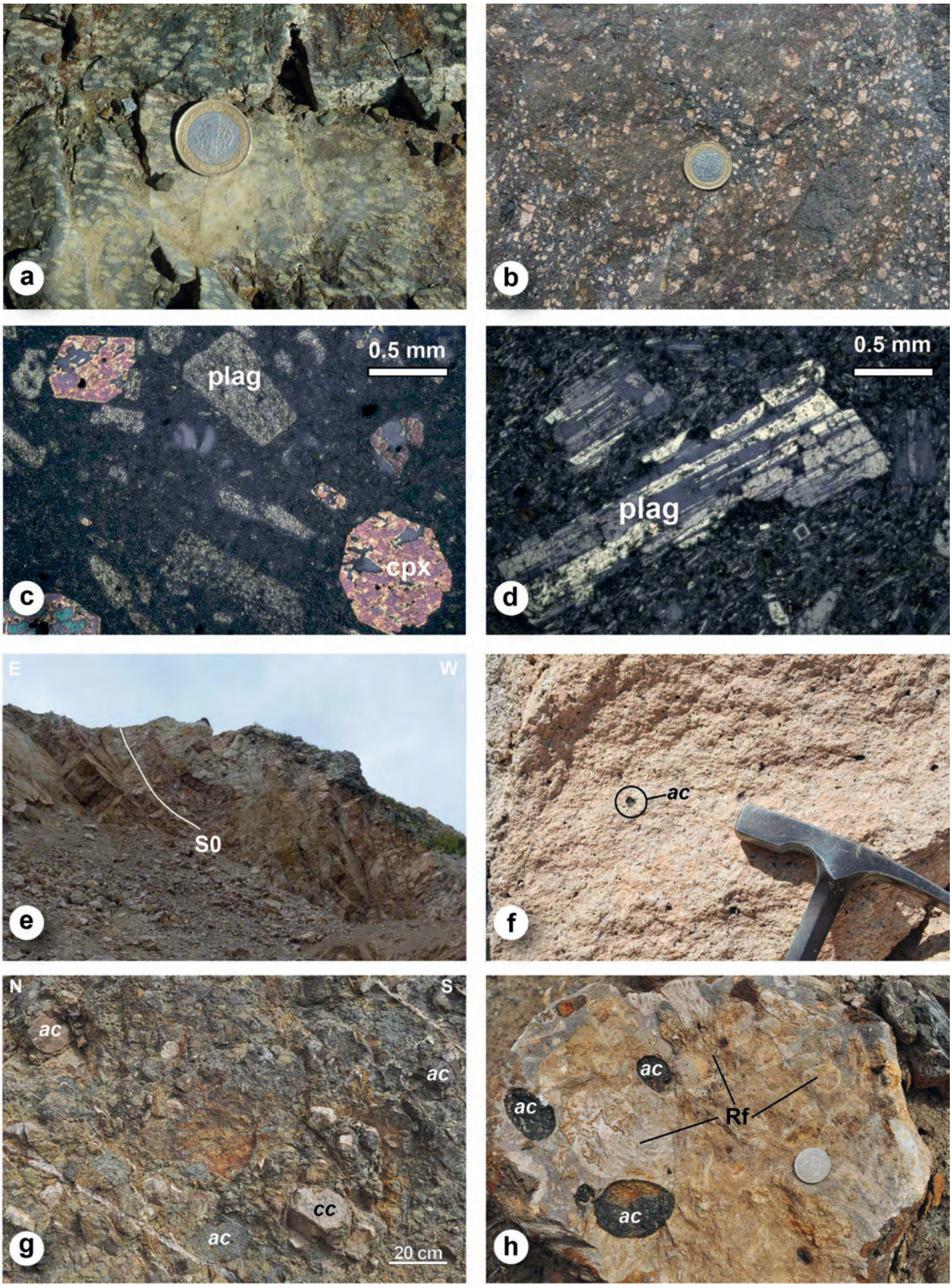

Fig. 4 - Field occurrence and petrographic features of the Tafano unit volcanic sequence. a) and b) porphyritic basaltic andesites with visible plagioclase phenocrysts embedded in a fine-grained matrix; c) photomicrograph of a plagioclase porphyric basaltic andesites; d) photomicrograph of a clinopyroxene-plagioclase porphyric andesites (plag: plagioclase; cpx: clinopyroxene); e) and f) field occurrence of the calcarenites lithofacies; g) and h) volcanic/carbonatic breccia of the Volcanoclastic Sandstone Formation. S0: bedding. ac: volcanic fragment. cc: carbonatic fragment. Rf: rudist fragment.

Lithostratigraphic features

The lithostratigraphic features of the Tafano unit have been reconstructed in the almost uninterrupted section cropping out along the road from Tosya to Çankırı, between GPS coordinates N40° 50.854', E33° 57.725' and N40° 48.839', E33° 56.413' (Fig. 2).

The lithostratigraphic succession is characterized by an estimated thickness of about 3,600 m (Fig. 3). It starts with volcanic rocks of about 800 m in thickness, cropping out between Aşağiöz, to the west and Söğnük, to the east (Fig. 2), consisting of basalt-basaltic andesite flows and their pyroclastic equivalents occuring mainly as agglomerates (Fig. 4a-d). Basaltic dikes and sills also occur. Intercalated in the andesites, calcarenites and calcirudites occur (Fig. 4e), characterized by coeval carbonatic platform and minor volcanic clasts, even evident at the macroscopic scale (Fig. 4f). These calcarenites and calcirudites (Calcarenite lithofacies) form a huge body alternated into the volcanic rocks, testifying the erosion of a carbonatic platform probably developed onto the volcanic arc during a lull in volcanic activity. The deposits overlying the volcanic rocks constitute the Volcaniclastic Sandstone Formation (Fig. 3). The lowermost part of this formation is made up by breccias showing cm to dm clasts of volcanics and limestones embedded within a siltitic matrix (Fig. 4g). The carbonatic clasts are fossiliferous limestones charaterized by large bivalves, probably rudists, associated to well-rounded grains of volcanics (Fig. 4h). These observations suggest a depositional evolution characterized by a first stage of shallow-marine setting for the fossiliferous limestones, followed by a redeposition in a subaerial setting for the breccias overlaying the volcanic rocks.

The sedimentary succession continues upwards with a turbidite sequence of medium to coarse-grained arenites and siltites alternating with grey marls and marly-siltitic shales (Fig. 5a-b). The bedding thickness ranges from centimetric to metric. Ripples, groove and tool marks are common at the base of the beds, while the upper part is often characterized by intense bioturbation.

The Volcaniclastic Sandstone Formation is also characterized by the occurrence of pebbly mudstones with clasts of quartz and carbonate rocks. Peculiar geological features such as ball-sized sandstone/siltstone concretions occur frequently. Overall, the detritic formation overlaying the volcanic rocks reaches about 800 m in thickness.

The sedimentary sequence ends with the Marly-calcareous Turbidite Formation, a thick succession (maximum exposure about 2,000 m) of calcareous turbidites and megaturbidites (Fig. 5c-d). The turbidite beds are composed by limestones (calcarenites, calcisiltites and calcilutites) locally intercalated with arenaceous-pelitic turbidites supply from the volcanics. Frequently, the beds are characterized at the base by arenites followed by massive grey marls and calcareous marls (Fig. 5e), bearing rests of *Inoceramus* (Fig. 5f).

Sandstone petrography

In order to characterize the petrography of the Tafano unit sedimentary rocks and the main features of its provenance area, one sample from the Calcarenite lithofacies, four samples from the Volcaniclastic Sandstone Formation and seven samples from the Marly-calcareous Turbidite Formation have been studied under polarizing microscope (see Fig. 3 for sample location in the stratigraphic log).

The Calcarenite lithofacies (Fig. 6a) is characterized by an intrabasinal carbonatic composition (calcarenites sensu Zuffa, 1980). The dominant rock fragments are derived from the reworking of a coeval carbonatic platform, which forms almost 100% of the arenite framework. The allochems are peloids, benthonic foraminifera and macrofossil fragments often represented by rudists. Minor volcanic rock fragments (basaltic andesite and andesite) can be also recognized as well as monocrystalline zoned plagioclase and clinopyroxene (Fig. 6a).

Arenites from the Volcaniclastic Sandstone Formation are almost pure volcaniclastic lithoarenites (Figs. 6b, c, d) locally bearing minor intrabasinal carbonatic fragments (up to 10% of the framework, can be sometimes recognized). The volcanic rock fragments are basaltic-andesites, andesites and minor dacites and rhyolites. Moreover, monocrystalline volcanic-derived fragments, such as plagioclase, sanidine, clinopyroxene and minor olivine, amphibole, quartz and oxides are common and characterize almost all the framework of the more fine-grained arenites.

The most striking feature of these arenites is the presence a "monogenous" volcanic debris composition such as the arenites are made of only one type of volcanic rocks (Fig. 6b, c, d). This "monogenous" composition suggests a source area located close to the basin margin or even inside it and a coeval origin of the volcanic rock fragments.

The arenites from the Marly-calcareous Turbidite Formation are lithoarenites characterized by a mixed siliciclastic-carbonatic composition (Fig. 6e, f). The arenites framework is a mixing of three different groups of rock fragments. The first and the second group belong to the intrabasinal and coeval volcanic and carbonatic platform rocks recognized in the Calcarenite lithofacies and in the Volcaniclastic Sandstone Formation. The volcanic rock fragments mainly derived from basaltic andesites, andesites and rhyolites, while in the coeval carbonatic rock fragments the association between *Orbitoides* and rudist fragments (Fig. 6g, h) indicate a Late Cretaceous age in agreement with the nannoplancton association recognized in this formation. The third group of rock fragments is characterized by the association of low grade metamorphic rocks (mainly micaschists and quartzites), intrusive magmatic rocks (granitoids) and sedimentary deep sea pelagic rocks (radiolaria bearing micritic wackestones and silicified wackestones). All these rock fragments have an extrabasinal and non-coeval origin and can be considered as representative of the uppermost part of a continental margin. According to Zuffa (1980) these arenites are a classical example of hybrid arenites, in fact they show a mixed carbonatic-siliciclastic and coeval-non coeval origin of its rock fragments framework.

To sum up the mixed/hybrid composition recognized in the analyzed corse-grained arenites and fine grained rudites points to a complex pattern characterized by three main source areas:

1- "Intrabasinal" and coeval volcanic rocks characterized the first source area. These rock fragments originated from a volcanic arc located close or even inside the sedimentary basin.

2- Intrabasinal and coeval carbonatic platform rocks. The intrabasinal carbonatic rock fragments can be recognized overall the sedimentary sequence, but were widespread in the Calcarenite lithofacies.

3- Mixed extrabasinal non-coeval silicilastic and carbonatic rocks derived from a continental upper crustal metamorphic and pelagic sedimentary sequences. This source area has been recognized only in the Marly-calcareous Turbidite Formation.

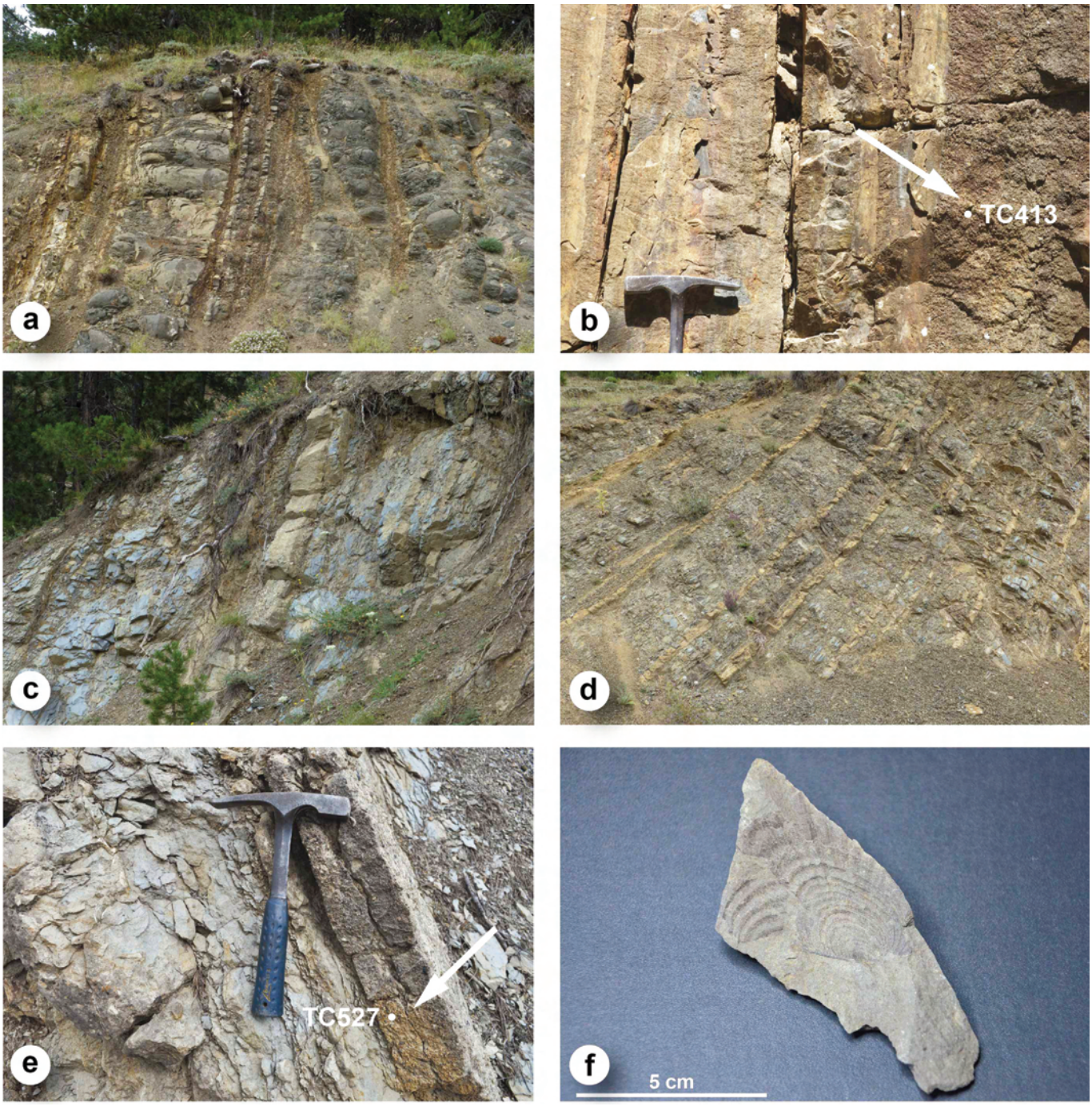

Fig. 5 - a) and b) Field occurrence of the Volcanoclastic Sandstone Formation. c), d) and e) Marly-calcareous Turbidite Formation. The white arrows indicate two sampled levels for arenites petrography; f) *Inoceramus* sp. from the upper part of Marly-calcareous Turbidite Formation.

Calcareous nannofossils

The age of the Tafano unit was performed using calcareous nannofossil biostratigraphy. A total of 77 samples were collected from outcrops reported in Fig. 3. The calcareous nannofossil content was studied on smear-slides prepared following standard procedures (Bown and Young, 1998) from unprocessed material through observation on optic microscope at 1250X.

46 samples were barren, whereas 31 contained calcareous nannofossil assemblages. The major part of the assemblages were impoverished and poorly preserved and allowed a generic "not older than" dating. Other samples documented specific time spans with the Sissingh's (1977) CC zones (Fig. 3).

The occurrence of *Arkhangelskiella confusa*, *Calculites obscurus* in assemblage with *Cribrosphaerella ehrenbergii, Eiffellithus gorkae, E. turriseiffelii, Micula staurophora, M. swastika, Prediscosphaera grandis, Quadrum gartneri, Reinhardtites antophorus, Retecapsa angustiforata, Tranolithus orionatus* and *Watznaueria* spp. testified the late Santonian CC17 Zone in the marly lithofacies of Volcaniclastic Sandstone Formation and in the lowermost part of the Marly-calcareous Turbidite Formation (samples BAT12-13, BAT13-13, BAT 18-13, BAT 21-13, BAT 27-13) (Fig. 7).

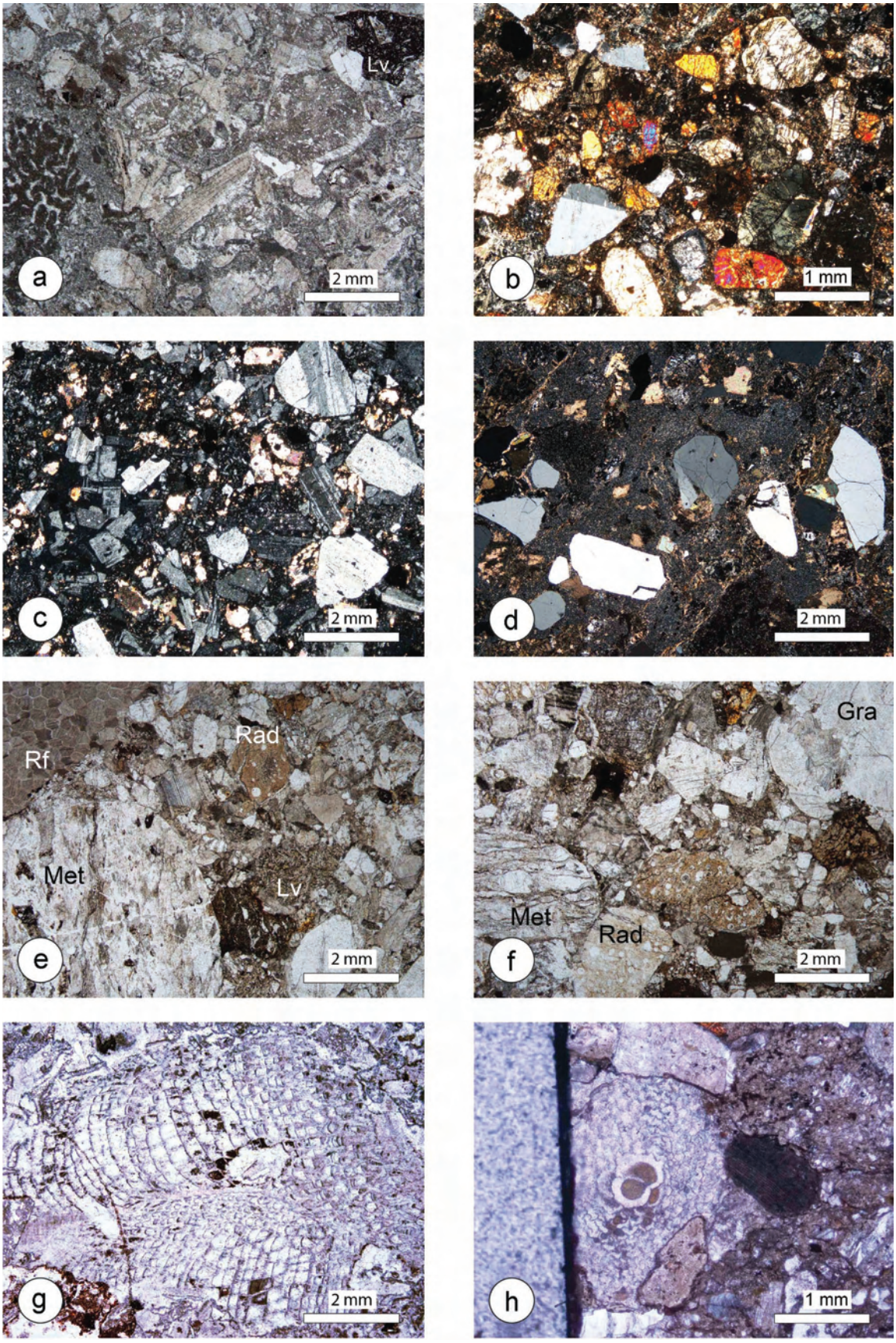

Fig. 6 - Petrographic features of the Tafano unit sedimentary cover. a) photomicrograph of the arenites from Calcarenite lithofacies. Sample BAT1513. (Lv: volcanic fragment). Volcaniclastic Sandstone Formation: b) lithoarenites dominated by andesite-basalt fragments, c) lithoarenites dominated by dacite-andesite fragments and d) lithoarenites dominated by rhyolite fragments. e), f) Marly-calcareous Turbidite Formation, aspect of the arenite petrofacies (Met: low-grade metamorphic rock fragment; Rad: radiolarian bearing wackestones and siliceous shale; Lv volcanic rock fragment; Rf: Rudista fragment; Gra: granitoids. g) Rudista and h) Orbitoides fragments in the rudites and arenites of the Marly-calcareous Turbidite Formation.

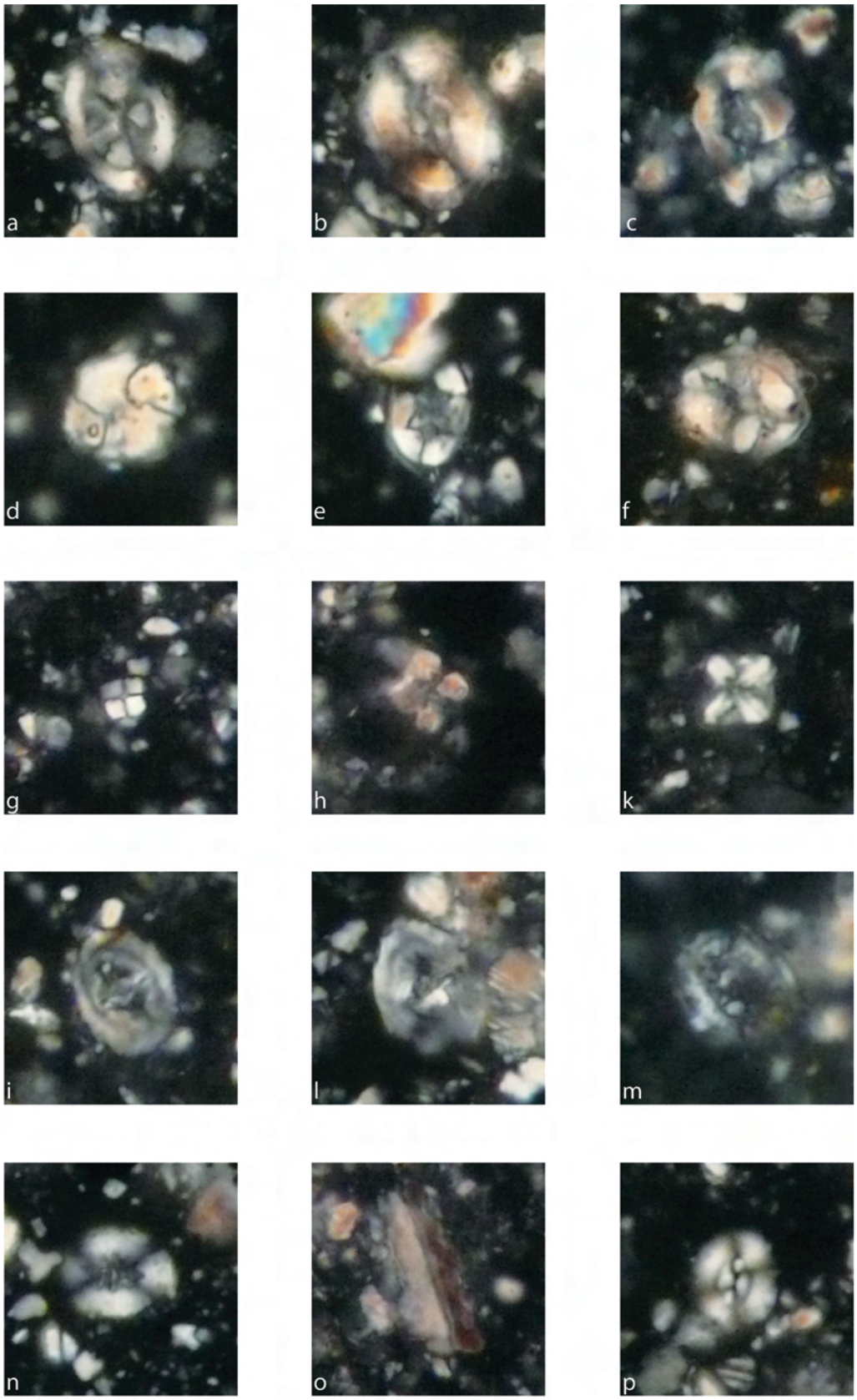

Fig. 7 - Photomicrographs of selected nannofossils derived from the Tafano unit succession. Optic microscope, 1250 magnifications, crossed polar. a) *Arkhangelskiella confusa* (sample BAT18-13); b) *Aspidolithus parcus constrictus* (sample BAT33-13); c) *Aspidolithus parcus parcus* (sample AET48); d) *Calculites obscurus* (sample BAT18-13); e) *Eiffellithus turriseiffelii* (sample BAT21-13); f) *E. eximius* (sample BAT33-13); g) *Quadrum gartneri* (sample BAT12-13); h) *Q. gothicum* (sample AET44); k) *Micula staurophora* (sample BAT13-13); i) *Reinhardtites anthophorus* (sample BAT18-13); l) *R. levis* (sample AET50); m) *Cribrosphaerella ehrenbergii* (sample BAT21-13); n) *Retecapsa angustiforata* (sample BAT18-13); o) *Lucianorhabdus* (sample AET44); p) *Watznaueria barnesae* (sample BAT13-13).

The appearance of *Aspidolithus parcus constrictus* associated with *Calculites obscurus*, *Cribrosphaerella ehrenbergii*, *Micula* spp., *Reinhardtites antophorus* and *Watznaueria* spp. allowed the identification of early Campanian CC18 Zone in the middle part of the Marly-calcareous Turbidite Formation (samples BAT30-13, AET39).

The occurrence of *Quadrum gothicum* with *Aspidolithus parcus parcus*, *Micula* spp., *Reinhardtites levis*, *R. anthophorus*, *Tranolithus phacelosus* and *Watznaueria* spp. allowed the identification of middle Campanian CC21 Zone in the upper part of the Marly-calcareous Turbidite Formation (samples AET48, AET50) (Fig. 7).

The calcareous nannofossils content suggests a late Santonian to middle Campanian age for the Tafano unit (Fig. 3). In literature, a younger Maastrichtian age, based on planktonic foraminifera, was reported for the Yaprakli Formation (Tüysüz et al., 1995; Rice et al., 2006). The Yapraklı Formation can be approximatively correlated with the Marly-calcareous Turbidite Formation of the Tafano unit. However the planktonic foraminifera assemblage described by Tüysüz et al., 1995, has a wider distribution, featuring the interval of time between the middle Campanian *Globotruncana calcarata* to early Maastrichtian *Gansserina gansseri* Zones (see assemblages reported in Chacón et al., 2004). Therefore, in our study the nannofossil analyses refine to a more specific time span the age of the Marly-calcareous Turbidite Formation.

Petrography and geochemistry of the volcanic rocks

The lavas of the Tafano unit are basalts to basaltic-andesites. All samples are strongly porphyritic with phenocrysts (visible by naked eye) set in a fine-grained matrix. Clinopyroxene and plagioclase are the dominant phenocryst phases. Olivine (now completely altered) represents a minor phenocryst phase. Rarely, leucite (altered to analcime) occurs as a phenocryst phase in some samples. Some samples show vitrophyric texture, indicating rapid cooling.

Clinopyroxene is represented by colorless to pale-green diopsidic augite. In some samples, it is fresh with well-developed cleavage and twinning (mostly simple twins). In some cases, however, it is partially or completely altered by secondary chlorite and calcite. Fresh plagioclase is characterized by lath shaped crystals with typical polysynthetic twinning (combined twins also exist). The composition of the plagioclase phenocrysts appears to be labradorite. Groundmass plagioclase forms flow texture in some samples. In general, plagioclase is variably altered by secondary phases, such as sericite (being the most common), calcite, chlorite and zeolite. No fresh olivine exists and it occurs as completely replaced crystals by serpentine, chlorite and calcite. Some samples show vesicular texture with chlorite and zeolite. Groundmass is generally altered by chlorite. Carbonatization and oxidation of the groundmass also occurs.

Eight selected samples were analyzed for major and trace elements (including REE). The whole-rock geochemistry analyses were performed in the ACME Labs (Canada). Major elements were measured by inductively coupled emission spectrometry (ICP-ES) and trace elements were determined by inductively coupled plasma mass spectrometry (ICP-MS). The geochemical data are presented in Table 1.

The Tafano lava samples display loss on ignition values ranging between 2.4-6.3 wt%, which may suggest that the samples have undergone some degree of alteration. Under such conditions, the pristine geochemistry may be disturbed owing to the mobile behaviour of some elements, such as Ba, Rb and K. In contrast, high field strength elements (HFSE) and rare earth elements (REE) are generally immobile under post magmatic processes and their concentrations are largely preserved (e.g., Pearce, 1975; Staudigel et al., 1996). When Zr is plotted against major and trace elements, it can be inferred that low-ionic potential elements (e.g., Ba, Rb and K) have been partly mobilized, while HFSE and REE appear to have remained largely immobile (not shown). This idea is also supported by the behaviour of these elements against loss on ignition (LOI), where concentrations of low-ionic potential elements have changed along with LOI contents in some samples, suggesting that element mobilization has occurred in some samples. Thus, the petrogenetic interpretations will be mainly based on the HFSE and REE, while LILE will be used with caution.

The Tafano samples range in composition from basalt to andesites and they are all characterized by sub-alkaline characteristics on the basis of Nb/Y ratios ranging between 0.4-0.6 (Fig. 8). When the K_2O contents are considered, however, the Tafano lavas are akin to shoshonitic lavas (Peccerillo and Taylor, 1976). They have moderate Zr/Nb ratios (10.1-15.6) when compared to those of normal mid-ocean ridge basalt (N-MORB) and oceanic island basalt (OIB) (31.8 and 5.8, respectively; Sun and McDonough, 1989). The Tafano lavas appear to be highly enriched in Th (7.7-17.1 ppm; average Th in N-MORB = 0.12 ppm; Sun and McDonough 1989). In N-MORB-normalized multi-element variation plots (Fig. 9a), the samples show prominent negative Nb anomalies with relative enrichment of Th and La over Nb (Th/Nb = 1.2-1.7, La/Nb = 1.9-3.7; La/Nb in N-MORB = 1.1). All Tafano lavas are characterized by Ti, Y and Yb contents which are comparable or slightly depleted with respect to that of average N-MORB. Most of the samples display negative Ti anomalies. Three samples exhibit Zr-Hf depletion, reflecting lower Zr/Nd (3.3-4.3) and Hf/Sm (0.4-0.5) ratios relative to others (5.3-6.9 and 0.7-0.8). In chondrite-normalized REE plots (Fig 9b), the Tafano lavas are relatively enriched in LREE over HREE ($[La/Yb]_N$ = 7.4-12.8). HREE in these samples are relatively unfractionated and they reflect flat patterns ($[Dy/Yb]_N$ = 1.1-1.4).

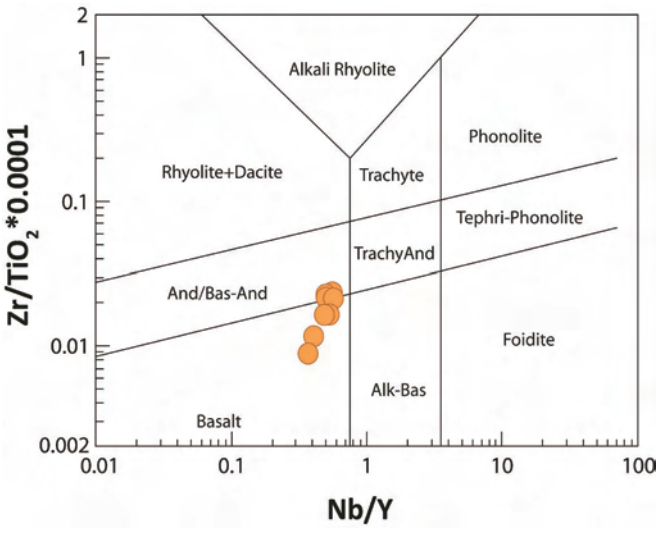

Fig. 8 - Chemical classification of the Tafano lavas (after Winchester and Floyd, 1977, modified by Pearce, 1996). (Alk-Bas: alkali basalt; And: andesite; Bas-And: basaltic andesite; TrachyAnd: trachy andesite).

Table 1 - Geochemical data of the studied volcanic rocks from the Tafano unit.

Sample	AET-13	AET-16	AET-17	AET-20	IPS-13-59	IPS-13-65	IPS-13-67	IPS-13-79
SiO2	51.18	52.26	48.86	49.35	56.42	51.90	51.55	44.93
Al2O3	17.72	17.40	20.56	20.44	16.53	17.04	18.04	17.79
Fe2O3	8.80	8.40	9.43	9.19	8.26	8.63	7.77	10.57
MgO	4.27	4.25	2.56	2.54	4.42	4.25	4.35	5.11
CaO	5.74	5.10	8.73	8.61	3.99	5.48	6.88	6.53
Na2O	3.01	3.16	3.10	3.14	3.77	3.59	3.54	5.29
K2O	4.80	5.01	2.71	2.74	0.34	4.19	3.78	1.61
TiO2	0.75	0.74	0.73	0.73	0.62	0.74	0.80	0.81
P2O5	0.33	0.31	0.31	0.32	0.23	0.31	0.34	0.45
MnO	0.12	0.11	0.15	0.17	0.05	0.11	0.12	0.22
Cr2O3	0.002	0.002	b.d.	b.d.	0.012	0.004	0.005	0.007
LOI	2.9	2.8	2.5	2.4	5.0	3.4	2.5	6.3
Sum	99.56	99.57	99.66	99.65	99.61	99.65	99.69	99.60
Ni	9.2	9.9	4.4	3.8	21.1	9.2	11.4	17.2
Co	22.9	24.4	24.8	25.7	31.8	27.2	26.3	34.4
Sc	23	22	13	12	15	22	24	23
V	217	216	167	158	154	208	208	302
Rb	118.0	120.4	62.9	64.8	4.4	94.0	80.6	67.8
Sr	1338.7	1361.1	669.6	688.7	319.6	1050.7	676.1	820.0
Ba	956	978	1028	1047	2180	672	711	1236
Hf	4.7	4.2	3.0	2.9	2.1	3.8	4.0	1.9
Nb	14.1	12.7	12.3	12.1	4.9	12.0	13.0	6.5
Ta	0.8	0.8	0.7	0.7	0.3	0.7	0.7	0.3
Zr	182.2	172.9	124.0	122.9	76.3	165.7	175.2	76.7
Y	25.2	25.3	23.1	24.8	12.0	23.9	22.8	17.5
La	32.4	31.0	41.6	40.6	14.4	26.7	24.4	23.8
Ce	59.4	57.2	69.8	72.3	31.0	52.6	52.0	47.4
Pr	7.05	6.66	8.03	8.07	3.44	6.04	6.35	5.64
Nd	27.5	26.5	29.0	30.8	14.4	24.1	25.9	23.5
Sm	5.66	5.33	5.69	5.64	2.89	5.10	5.20	4.79
Eu	1.37	1.38	1.49	1.54	0.79	1.25	1.25	1.22
Gd	5.58	5.25	5.15	5.16	2.62	4.79	5.02	4.29
Tb	0.80	0.77	0.75	0.72	0.40	0.71	0.76	0.59
Dy	4.69	4.52	4.30	4.25	2.23	4.24	4.32	3.23
Ho	0.87	0.87	0.84	0.79	0.47	0.88	0.81	0.63
Er	2.69	2.54	2.39	2.44	1.36	2.38	2.45	1.57
Tm	0.40	0.38	0.36	0.34	0.19	0.37	0.36	0.25
Yb	2.67	2.58	2.33	2.37	1.32	2.46	2.38	1.54
Lu	0.43	0.41	0.36	0.35	0.20	0.37	0.40	0.24
Th	17.1	16.4	14.7	14.8	8.3	15.5	15.6	7.7
U	6.9	6.6	3.9	3.5	1.6	4.8	6.2	3.2
Pb	13.8	15.8	7.0	6.6	5.5	13.1	6.8	7.3

Deformation history

The Tafano unit experienced a complex deformation, even if the whole succession is not-metamorphic. The deformation pattern is the result of three main phases, referred as D_1, D_2 and D_3 phases, mainly identified in the sedimentary cover of the basal volcanic complex and in particular in the upper formation where the layered limestone and marl beds better reveal the structural evolution at the outcrop scale.

However, the D_1 phase is best expressed at the map scale (see geological cross-section B-B'; Fig. 2) by a kilometric sized isoclinal anticline showing the volcanic rocks at its core and folding the whole Tafano unit. In the field, the only evident D_1 structures are represented by a penetrative S_1 foliation parallel to S_0 bedding. The S_0-S_1 surface is deformed by D_2 folding phase (Fig. 10a, c). The structures of the D_2 phase are characterized by asymmetric and overturned F_2 folds (Fig. 11a) with approximately parallel geometry (classes 1b, 1c of Ramsay, 1967). The hinges of the F_2 folds are commonly rounded, the interlimb angles range from 70° to 120° (open folds), and the axial planes are generally low-angle dipping surfaces. The D_2 folding produced a well developed axial-plane foliation S_2 (Fig. 10b, d) that can be classified as disjunctive cleavage. This disjunctive cleavage developed inside limestones as well as inside marls and sandstones showing a spaced convergent fanning. Locally, the S_0-S_1/S_2 intersection lineations originated a typical pencil cleavage (Fig. 11b). The F_2 fold axes are directed NE-SW.

Afterwards, the Tafano unit has been affected by a later third phase of deformation, D_3, essentially represented by brittle faulting. D_3 phase produced mainly high angle faults that represent also the boundaries of the Tafano unit with the surrounding blocks composed by the deposits of the Arkot Dağ Mélange (Fig. 2).

The structural analysis at the mesoscale allowed to measure 64 fault planes represented almost exclusively by high angle faults that can be subdivided into two main systems trending roughly E-W and NNE-SSW, respectively (Fig. 12). According to the plunge angles of the detected slickensides, the faults are predominantly strike-slip faults (Fig. 12a). The

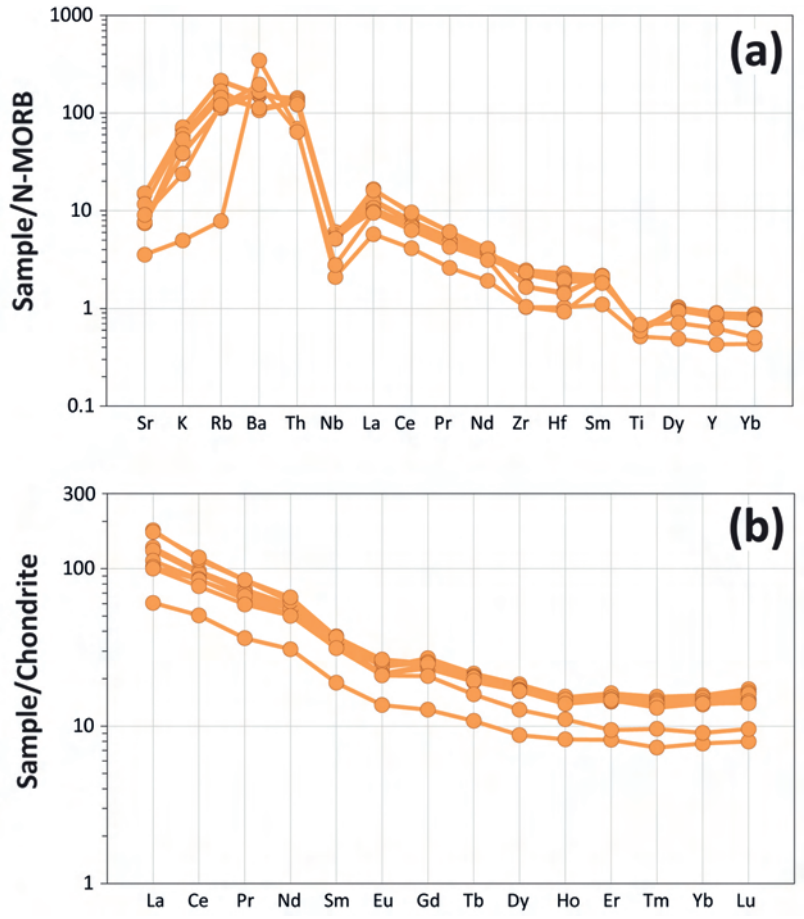

Fig. 9 - a) Trace element and b) REE patterns of the Tafano lavas. Normalization values from Sun and McDonough (1989).

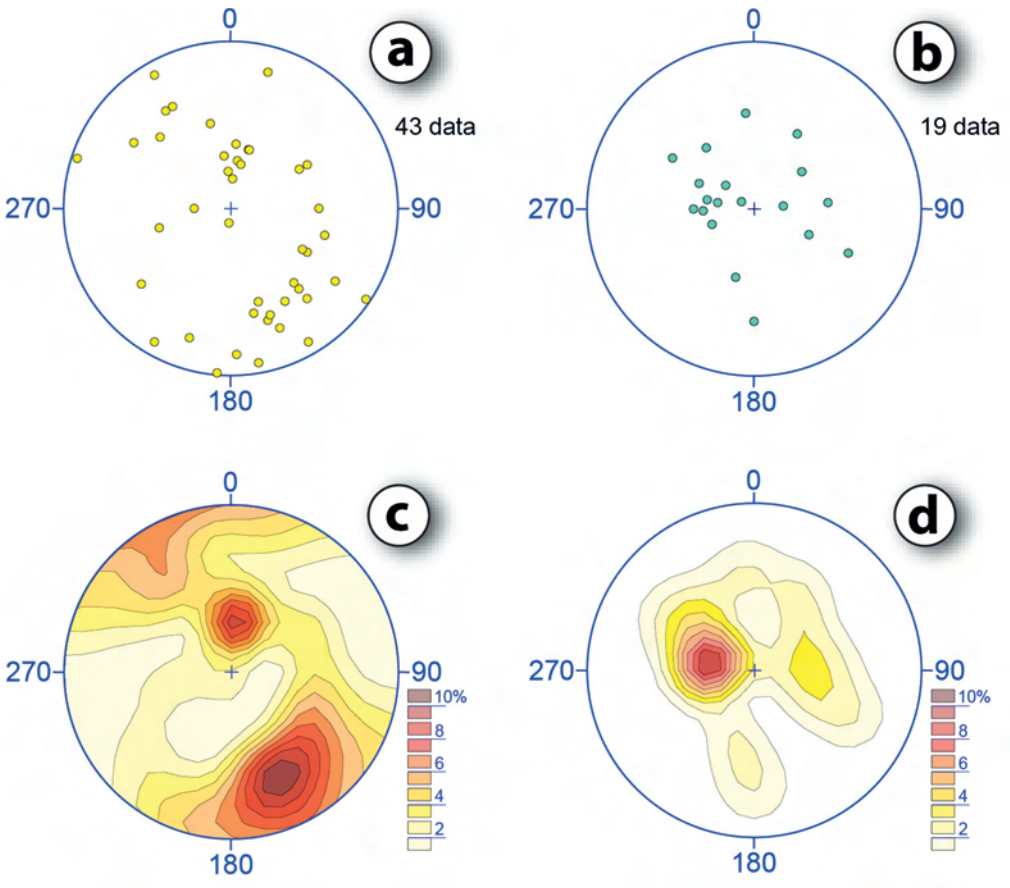

Fig. 10 - Equal-area, lower hemisphere stereographic representation of D_1 and D_2 structural data. a) S_0-S_1 surfaces poles distribution and c) contour plot. b) S_2 foliation poles distribution and d) contour plot.

occurrence of multistriated fault planes indicate that the D_3 phase is characterized by a complex evolution including different superposed steps of deformation (Fig. 11c, d). Multi-structure braided shear zone systems have been observed (Fig. 11e), including strike-slip faults, metric shear-zone, positive flower structures and bedding-parallel shear surfaces.

The kinematic analysis allowed defining two conjugate systems of strike-slip faults, both characterized by roughly E-W and NNE-SSW directions, with alternate dextral and sinistral sense of movement (Fig. 13). Consequently, the paleo-stress reconstruction suggests the occurrence of two different strike-slip tensors, displaying a NW-SE and SW-NE trending σ1 maximum compressive stress axes, respectively.

A clear cross-cutting relationship between the two coniugate fault systems was not observed during the field structural analyses. However, the NW-SE trending σ1 system can be easily correlate with the main North Anatolian shear zone (Ellero et al., 2015). The second fault system

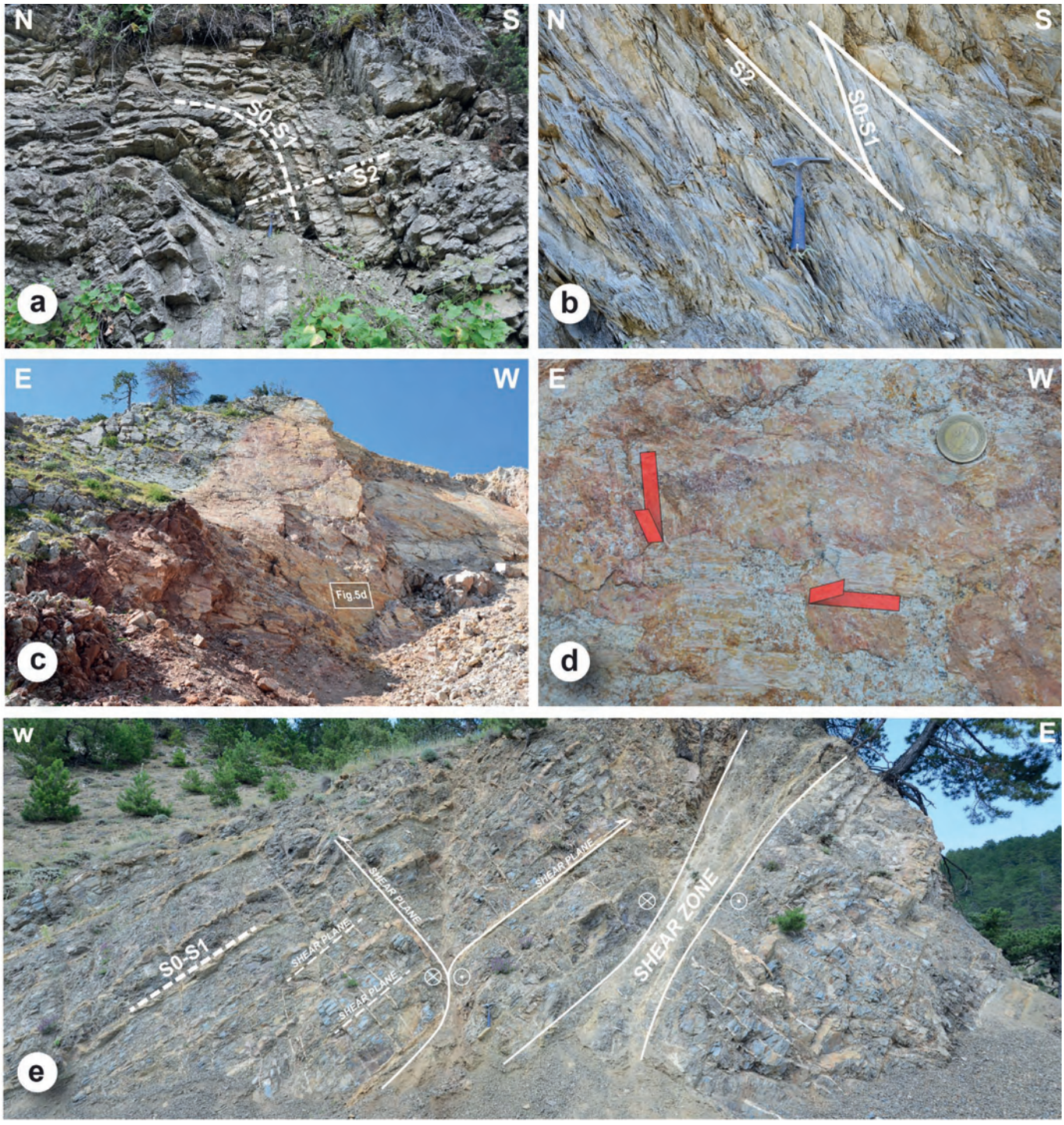

Fig. 11 - Geometrical and kinematic features of Tafano unit. a) F_2 fold associated to a penetrative axial plane foliation S_2, developed in the Marly-calcareous Turbidite Formation. b) S_0-S_1/S_2 relationships with the development of pencil cleavage in the Marly-calcareous Turbidite Formation. c) High-angle fault developed in a calcarenite body alternated into the volcanic rocks. d) Detail of the fault plane, bearing two systems of slickenlines with dextral and normal senses of movement. The direction of the arrow corresponds to the movement of the missing block. e) Shear zone developed in the Marly-calcareous Turbidite Formation.

(SW-NE trending σ_1) is more difficult to interpret. Similar fault systems are described in the Çankırı Basin (Kaymakci et al., 2003). Comparing results from our paleostress inversion study with those by Kaymakci et al. (2003), an evolution of the brittle tectonics can be delineated in the study area including two main stages inside the D_3 deformation phase. The strike-slip regime with SW-NE trending σ_1, developing roughly E-W trending sinistral strike-slip faults, can be regarded as the older stage which has been ascribed to the late Paleocene-early Miocene age (Kaymakci et al., 2003). On the contrary, the strike-slip regime with NW-SE trending σ_1 seems to be younger, developing roughly E-W trending dextral strike-slip faults that can be regarded as expression of the late Miocene North Anatolian shear zone (Kaymakci et al., 2003).

DISCUSSION

The structural and stratigraphic studies in the area south of Tosya show that a roughly E-W elongated block bounded by high angle faults corresponds to a tectonic unit, informally denominated Tafano unit. The Tafano unit did not suffer metamorphism and displays stratigraphic boundaries among the three formations that make up the continuous succession of the unit, from the bottom: i) the Basal Volcanic Complex, including basalts to basaltic andesites, interrupted by a confined and brief episode of calcarenite deposition: the Calcarenite lithofacies; ii) the Volcaniclastic Sandstone Formation, including breccias and turbiditic sandstones and iii) the Marly-calcareous Turbidite Formation characterized by a mixed siliciclastic-carbonatic composition.

The qualitative petrographic analyses of the coarse-grained arenites and fine-grained rudites allowed delineating the evolution of the provenance areas feeding the sedimentary cover of the Tafano unit. The age of this sedimentary cover is constrained by the nannofossil assemblages to the late Santonian-middle Campanian. The lowermost part was fed by a mixed carbonatic-volcaniclastic intrabasinal source area. The debris mainly derived from the reworking of the volcanic rocks that characterized the basement of the Tafano unit and by coeval carbonate platforms developed at the top

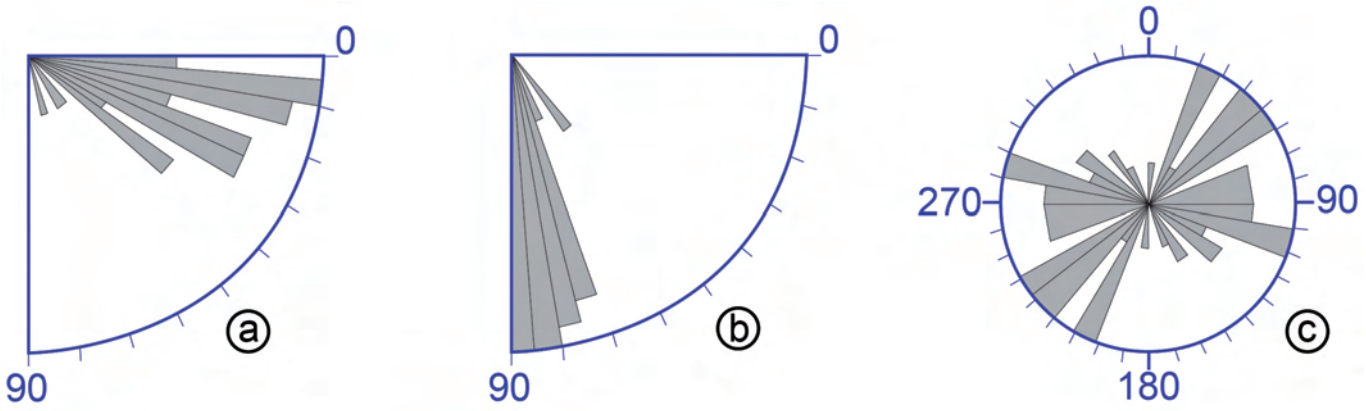

Fig. 12 - Statistical analysis of structural data from the fault systems of the Tafano unit. Rose diagrams showing plunge of slickensides (a) and dip (b) and strike (c) of faults. Total fault number: 64.

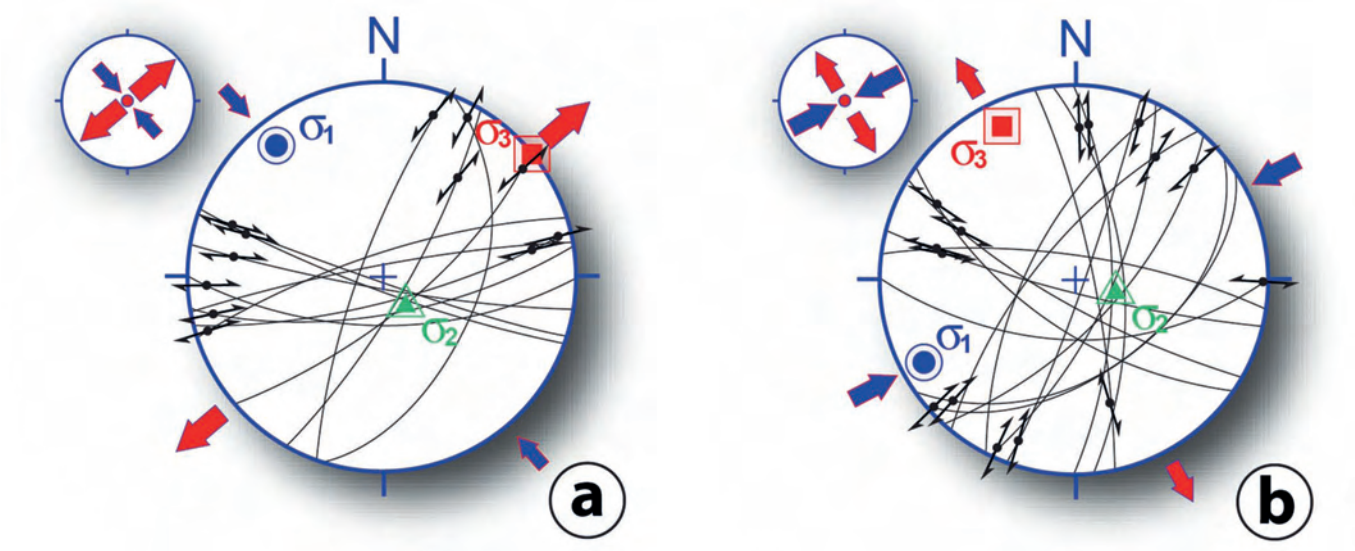

Fig. 13 - Stereograms showing traces of strike-slip faults with observed slip lines and slip senses (equal-area stereographic projections, lower hemisphere) from the Tafano unit. The principal stress axes (σ_1, σ_2, σ_3) and type of stress tensor were obtained using the Win_TENSOR software (Delvaux and Sperner, 2003). (a) Tensor data: σ_1 15/321, σ_2 75/147, σ_3 02/051, R 0,80; fault number: 12. (b) Tensor data: σ_1 13/241, σ_2 71/108, σ_3 13/335, R 0,35; fault number: 16.

of the volcanic complex. In the Marly-calcareous Turbidite Formation a continental margin-derived source area starts to influence the debris composition even if the more important one still remain the mixed carbonatic-volcaniclastic intrabasinal source area.

Whole-rock geochemical analyses have been performed in order to define the tectono-magmatic framework of the volcanic rocks of the Tafano unit. The analyzed volcanics display Zr/Nb ratios in the range of 10.1-15.6. These values are lower than that of N-MORB (31.8; Sun and McDonough 1989), which are regarded to have been largely derived from the depleted portions of the upper mantle (depleted MORB mantle, DMM; Zindler and Hart, 1986; Allègre, 1987). Thus, the moderate Zr/Nb ratios of the Basal Volcanic Complex lavas may suggest that they have not been derived dominantly from DMM, but also have involved enriched sources in their petrogenesis. In addition, low-degrees of partial melting may have also played a role on creating Zr/Nb ratios lower than that of N-MORB.

The Basal Volcanic Complex lavas display marked Th enrichment relative to Nb. This feature is typical of magmas generated in the subduction zones (Hawkesworth et al., 1993; McCulloch and Gamble, 1991; Pearce, 2008; Saccani, 2015). During the subduction of oceanic lithosphere, some elements (e.g., LILE, LREE) are removed from the crust via fluids and melts, which subsequently metasomatize the overlying mantle wedge (Pearce and Peate, 1995; Tatsumi and Kogiso, 2003). Some others (i.e. HFSE and HREE), however, are retained in the crust owing to their low solubility and the presence of some accessory phases (e.g., rutile), thus they have negligible effect on the composition of the mantle wedge (Pearce and Peate, 1995). Apart from these Ti-rich accessory phases on the oceanic crust, mantle amphibole has also been proposed to be capable of effectively partitioning Nb and Ta (Ionov and Hofmann, 1995). Consequently, the melts produced from such modified mantle source are characterized by relative enrichment in LILE and LREE over HFSE and HREE. The high Th/Nb and La/Nb ratios, therefore, may suggest that the Basal Volcanic Complex lavas have derived from a mantle source that had been metasomatized by slab-derived fluids and/or melts.

The idea of the presence of subduction component in the Basal Volcanic Complex samples can also be tested by using trace element ratios, Nb/Yb and Th/Yb (Pearce 1983; Pearce and Peate, 1995) (Fig. 14). Of these elements, Nb and Yb are subduction-immobile (Pearce and Stern, 2006), thus these elements will not be mobilized from the subducted slab neither via fluids nor melts. Th, on the other hand, can partition into melt phase, and subsequently transferred to the mantle wedge. In the plot of Nb/Yb vs Th/Yb, the melt compositions derived from a mantle source with no slab-derived addition (i.e. MORBs and most OIBs) will be distributed along an array known as MORB array. In contrast, a mantle source including subduction component would create melts whose compositions will be plotted off the array owing to the Th addition from the slab. In the plot, the Tafano samples are observed to be displaced above the array, suggesting the contribution of subduction component in the mantle source of these lavas (Fig. 14).The REE systematics of the Basal Volcanic Complex lavas reflect LREE-enriched profiles with a rather flat pattern. While the LREE enrichment can be caused by subduction enrichment and/or relatively small degrees of partial melting, the somewhat unfractionated patterns of HREE (which are subduction immobile) may suggest that the Basal Volcanic Complex samples have derived dominantly from a mantle source where spinel was stable (i.e. spinel lherzolite).

In summary, the trace element systematics of the volcanic rocks suggest that they have been generated from a mantle source modified by subduction component, which created high Th/Nb and La/Nb ratios. Such characteristics are typically found in arc-related lavas (Peate et al., 1997; Jolly et al., 2001; Calanchi et al., 2002; Stern et al., 2006). One possibility is that the Basal Volcanic Complex lavas have originated in an oceanic arc system (i.e. island arc), similar to what was proposed for other tectono-magmatic units in the south of Tosya (Tüysüz et al., 1995; Rice et al., 2006; Aygül et al., 2015b). Solely based on geochemistry, the somewhat enriched character of the Tafano (moderately high Zr/Nb and Nb/Yb ratios) samples seem to be somewhat against this idea, since oceanic arc magmas generally display depleted geochemical signatures (Pearce and Peate, 1995). The Basal Volcanic Complex samples, instead, are rather akin to the magmas formed at the continental arcs (De Astis et al., 1997; Bryant et al., 2006). The relative enrichment in Nb compared to N-MORB, and LREE-enriched characteristics are the features common in this tectonic setting, which can be attributed to the involvement of continental crust and/or lithospheric mantle (Pearce, 1983; Calanchi et al., 2002; Mamani et al., 2010). This idea is also reinforced by the Th-Nb systematics proposed by Saccani (2015) (Fig. 15). Therefore, the geochemical signatures of the Tafano lavas are rather consistent with an origin of these lavas from an active continental margin.

This interpretation is supported by the sandstone petrographic analysis data, pointing to a clastic component derived from a continental margin in the upper formation of the Tafano unit succession.

The identification of a tectonic unit, the Tafano unit, resulting from an active continental margin, raises the issue of where to place this margin within a regional geodynamic scenario.

The paleogeographic reconstructions referred to the study area provide one oceanic branch of the Neo-Tethys coinciding with the IAES (Tüysüz et al., 1995; Aygül et al., 2015b).

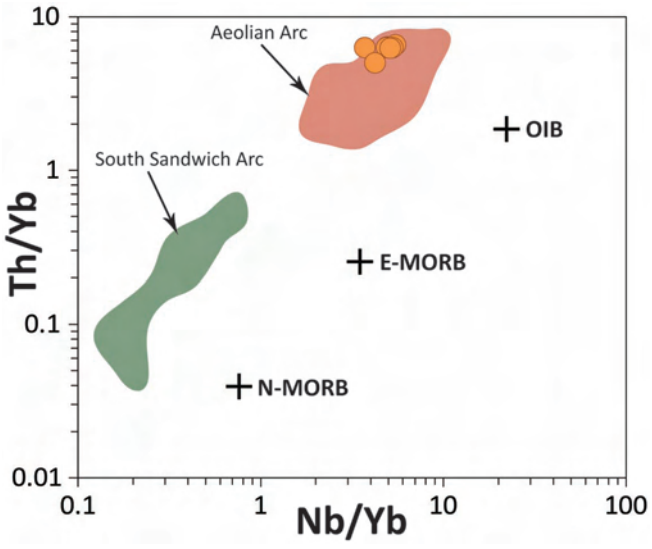

Fig. 14 - Nb/Yb vs Th/Yb plot. South Sandwich data from Pearce et al. (1995). Aeolian data from Calanchi et al. (2002). Concerning the published data, the samples whose MgO content is less than 2 wt.% have been excluded for comparative purposes.

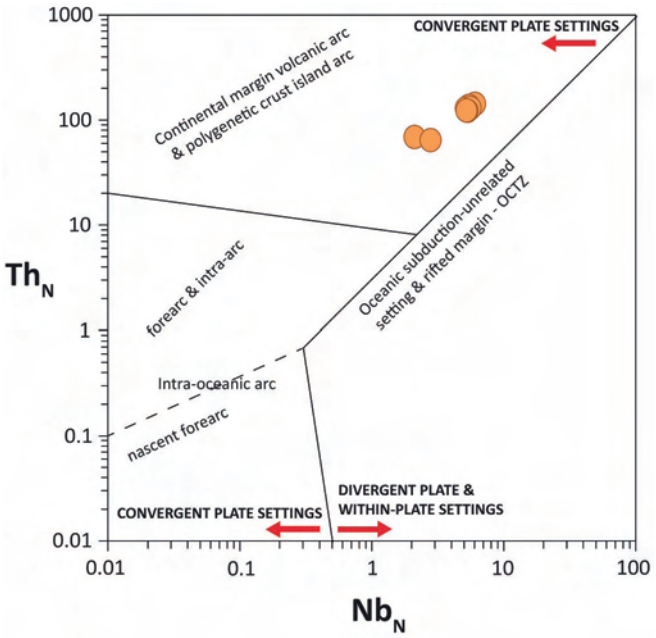

Fig. 15 - Th_N-Nb_N plot of the Tafano lavas (after Saccani, 2015).

According to this model, the Tafano unit could represent a continental arc and its sedimentary cover on the southern Sakarya terrane, generated in the northern active continental margin of the Izmir-Ankara-Erzincan ocean domain.

A variety of this model may involve the low-angle subduction of the Izmir-Ankara-Erzincan oceanic lithosphere beneath the Sakaria terrane, by which the continental arc (Tafano unit) develops at the northern margin of Sakaria terrane. By subsequent accretion of the Intra-Pontide mélange (cfr. Arkot Da Mélange) and their emplacement onto the passive margin of Sakaria terrane, the Tafano unit may have been imbricated with the Intra-Pontide suture zone units and finally gained its present structural alignment by the activities of the North Anatolian shear zone.

An alternative hypothesis suggests a continental arc related to the closure of the northernmost oceanic branch of the Neo-Tethys, represented by the Intra-Pontide oceanic basin (Marroni et al., 2014; Sayit et al., 2015). In this case, the Tafano unit could represent a slice derived from the Istanbul-Zongulfag terrane, the northern active continental margin of the Intra Pontide oceanic basin.

The geodynamic reconstruction of the Central Pontides is severely complicated by the overprint of the North Anatolian shear zone, dismembering the original structural stacking related to the closure of the oceanic domains. The fault zone activity generated a mosaic of fault bounded blocks, possibly juxtaposing tectonic units coming from different oceanic suture zones, Intra-Pontide or Izmir-Ankara-Erzinkan suture zones. The transcurrent component of the post-collisional geodynamic evolution of the Central Pontides, makes extremely complicated the paleogeographic reconstructions at regional scale, based only on the retrodeformation orthogonally oriented to the main belt trend.

CONCLUSIONS

A new tectonic unit, namely the Tafano unit, belonging to the Central Pontides - Northern Turkey has been described in the area between Tosya and the northern boundary of the Çankırı Basin. This unit consists of a volcanic complex covered by a late Santonian-middle Campanian sedimentary succession. The volcanic rocks display basaltic and basaltic-andesitic compositions with sub-alkaline nature. The volcanics are associated with volcaniclastic deposits evolving to marly-calcareous turbidites. The sedimentary succession is fed by three main source areas, constituted by a volcanic arc located close to the sedimentary basin, coeval carbonatic platform rocks and, in the Marly-calcareous Turbidite Formation, siliciclastic and carbonatic rocks derived from a continental upper crustal metamorphic and pelagic sedimentary sequences. The trace element systematics of the volcanics and the petrographic characteristics of the sedimentary succession points to an origin of the Tafano unit from an active continental margin. This active continental margin could be located in three possible alternative geodynamic settings within the Neo-Tethyan realm. The Tafano unit can be alternatively interpreted as belonging to north or south Sakaria or Istanbul-Zonguldag terranes, northern margins of Izmir-Ankara-Erzincan or Intra-Pontide oceanic domains respectively.

The assignment of the Tafano unit to one or other geodynamic setting needs more constraints, because it is hampered by the pervasive deformation related to the high angle faults belonging to North Anatolian shear zone. The effects of North Anatolian shear zone are clear in the Tafano unit and represent the more evident deformation phase in the field, with structures peculiar of a transcurrent tectonic regime. South of Tosya, the North Anatolian shear zone constitutes a deformation zone that extends for several kilometres, up to the northern boundary of the Çankırı Basin. In this wide deformation band, several blocks are juxtaposed, theoretically coming from domains also very far from each other. It is therefore possible to find in this zone units coming from different sectors of the Neo-Tethyan realm, namely Sakaria and Istanbul-Zonguldag terranes, and Izmir-Ankara-Erzincan and Intra-Pontide oceanic domains.

ACKNOWLEDGEMENTS

The authors gratefully acknowledge Mehmet Arslan and Emilio Saccani for their constructive reviews. The research has been funded by grants from MURST (PRIN 2010-11 project; resp. M. Marroni) and from IGG-CNR.

REFERENCES

Akbayram K., Okay A.I. and Satir M., 2012. Early Cretaceous closure of the Intra-Pontide Ocean in western Pontides (northwestern Turkey). J. Geodyn., 65: 38-55.

Allègre C.J., 1987. Isotope geodynamics. Earth Planet. Sci. Lett., 86: 175-203.

Andrieux J., Over S., Poisson A. and Bellier O., 1995. The North Anatolian Fault Zone: distributed Neogene deformation in its northward convex part. Tectonophysics, 243: 135-154.

Aydin M., Sahintürk O., Serdar H.S., Özçelik Y., Akarsu I., Üngör A., Çokuğraş R. and Kasar S., 1986. The geology of the area between Ballidağ and Çangaldağ (Kastamonu) (in Turkish). Bull. Geol. Soc. Turkey, 29: 1-16.

Aygül M., Okay A.I., Oberhansli R. and Ziemann M.A., 2015a. Thermal structure of low-grade accreted Lower Cretaceous distal turbidites, the Central Pontides, Turkey: insights for tectonic thickening of an accretionary wedge. Turk. J. Earth Sci., 24: 461-474.

Aygül M., Okay A.I., Oberhansli R., Schmidt A. and Sudo M, 2015b. Late Cretaceous infant intra-oceanic arc volcanism, the Central Pontides, Turkey: Petrogenetic and tectonic implications. J. Asian Earth Sci., 111: 312-327.

Barka A.A., 1992. The North Anatolian fault Zone. Ann. Tectonicae, 6: 164-195.

Berber F., 2015. Geology and petrology of the Kösedağ metavolcanic Rocks to the south of Tosya. M.S. Thesis. Middle East Techn. Univ., 120 pp.

Berber F., Göncüoğlu M.C. and Sayit K., 2014. Geochemistry and tectonic significance of the Kösedağ metavolcanic Rocks from the Sakarya Zone, Northern Turkey. In: Proceed. 20th CBGA Congr., Abstr. Book, 1: 161-163, Tirana, Albania.

Bortolotti V., Chiari M., Göncüoğlu M.C, Marcucci M., Principi G., Tekin U.K, Saccani E., Tassinari R., 2013. Age and geochemistry of basalt-chert associations in the ophiolitic complexes of the Izmir-Ankara Mélange, East of Ankara, Turkey: preliminary data. Ofioliti, 38: 157-173.

Bown P.R. and Young J.R., 1998. Techniques. In: P.R. Bown (Ed.), Calcareous nannofossil biostratigraphy. Kluwer Acad. Publ.,p. 16-28.

Bryant J.A., Yogodzinski G.M., Hall M.L., Lewicki J.L. and Bailey D.G., 2006. Geochemical constraints on the origin of volcanic rocks from the Andean northern volcanic zone, Ecuador. J. Petrol., 47: 1147-1175.

Calanchi N., Peccerillo A., Tranne C.A, Lucchini F., Rossi P.L., Kempton P., Barbieri M. and Wu T.W., 2002. Petrology and geochemistry of volcanic rocks from the island of Panarea: implications for mantle evolution beneath the Aeolian island arc (southern Tyrrhenian sea). J. Volcanol. Geotherm. Res., 115: 367-395.

Catanzariti R., Ellero A., Göncüoğlu M.C., Marroni M., Ottria G. and Pandolfi L., 2013. The Taraklı Flysch in the Boyalı area (Sakarya Terrane, Northern Turkey): Implications for the tectonic history of the Intrapontide Suture Zone. C. R. Geosci., 345: 454-61.

Chacón B., Martín-Chivelet J. and Gräfe K.-U., 2004. Latest Santonian to latest Maastrichtian planktic foraminifera and biostratigraphy of the hemipelagic successions of the Prebetic Zone (Murcia and Alicante provinces, south-east Spain). Creta. Res., 25: 585-601.

De Astis G., La Volpe L., Peccerillo A. and Civetta L., 1997. Volcanological and petrological evolution of Vulcano island (Aeolian Arc, southern Tyrrhenian Sea). J. Geophys. Res., 102: 8021-8050.

Dhont D., Chorowicz J., Yürür T. and Köse O., 1998. Polyphased block tectonics along the North Anatolian Fault in the Tosya basin area (Turkey). Tectonophysics, 299: 213-227.

Ellero A., Ottria G., Marroni M., Pandolfi L. and Göncüoğlu M.C., 2015. Analysis of the North Anatolian Shear Zone in Central Pontides (northern Turkey): insight for geometries and kinematics of deformation structures in a transpressional zone. J. Struct. Geol., 71: 124-141.

Elmas A. and Yiğitbaş E., 2001. Ophiolite emplacement by strike-slip tectonics between the Pontide Zone and the Sakarya Continent in northwestern Anatolia, Turkey. Int. J. Earth Sci., 90: 257-69.

Göncüoğlu M.C. and Erendil M., 1990. Pre-Late Cretaceous tectonic units of the Armutlu Peninsula. Proceed. 8th Turk. Petrol. Congr., 8: 161-168.

Göncüoğlu M.C., Dirik K. and Kozlu H., 1997. General Characteristics of pre-Alpine and Alpine Terranes in Turkey: Explanatory notes to the terrane map of Turkey. Ann. Géol. Pays Héllen. Geol. Soc. Greece, 37: 515-536.

Göncüoğlu M.C., Erendil M., Tekeli O., Aksay A., Kus I. and Ürgün B.M., 1987. Geology of the Armutlu Peninsula. In: Excurs. Guidebook, IGCP Project No. 5, 53 pp.

Göncüoğlu M.C., Gürsu S., Tekin U.K. and Koksal S., 2008. New data on the evolution of the Neotethyan oceanic branches in Turkey: Late Jurassic ridge spreading in the Intra-Pontide branch. Ofioliti, 33: 153-164.

Göncüoğlu M.C., Marroni M., Pandolfi L., Ellero A., Ottria G., Catanzariti R., Tekin U.K. and Sayit K., 2014. The Arkot Dağ Mélange in Araç area, central Turkey: Evidence of its origin within the geodynamic evolution of the Intra-Pontide suture zone. J. Asian Earth Sci., 85: 117-139.

Göncüoğlu M.C., Marroni, M., Sayit, K., Tekin U.K., Ottria G., Pandolfi, L. and Ellero, A., 2012. The Ayli Dağ ophiolite sequence (central-northern Turkey): A fragment of middle Jurassic oceanic lithosphere within the Intra-Pontide suture zone. Ofioliti, 37: 77-91.

Göncüoğlu M.C., Turhan N., Senturk K., Özcan A., Uysal S. and Yalınız M.K., 2000. A geotraverse across northwestern Turkey: tectonic units of the Central Sakarya region and their tectonic evolution. In: E. Bozkurt, J.A. Winchester and J.D.A. Piper., (Eds.), Tectonics and magmatism in Turkey and the surrounding area. Geol. Soc. London Spec. Publ., 173: 139-162.

Göncüoğlu M.C., Yalınız M.K. and Tekin U.K., 2006. Geochemistry, tectonomagmatic discrimination and radiolarian ages of basic extrusives within the Izmir-Ankara suture belt (NW Turkey): Time constraints for the Neotethyan evolution. Ofioliti, 31: 25-38.

Görür N., Monod O., Okay A.I., Sengör A.M.C., Tüysüz O., Yiğitbaş E., Sakınc M. and Akkök R., 1997. Palaeogeographic and tectonic position of the Carboniferous rocks of the western Pontides (Turkey) in the frame of the Variscan belt. Bull. Soc. Géol. France, 168: 197-205.

Gradstein F.M., Ogg J.G. and Smith A.G., 2004. A Geologic Time Scale 2004. Cambridge Univ. Press, Cambridge, 589 pp.

Hawkesworth C.J., Gallagher K., Hergt J.M. and McDermott F., 1993. Mantle and slab contributions in arc magmas. Ann. Rev. Earth Planet. Sci., 21: 175-204.

Ionov D.A. and Hofmann A.W., 1995. Nb-Ta-rich mantle amphiboles and micas: Implications for subduction-related metasomatic trace element fractionations. Earth Planet. Sci. Lett., 131: 341-356.

Jolly W.T., Lidiak E.G., Dickin A.P. and Wu T-W., 2001. Secular geochemistry of central Puerto Rican Island Arc lavas: Constraints on Mesozoic iectonism in the Eastern Greater Antilles. J. Petrol., 42: 2197-2214.

Kaymakci N., White S.H. and van Dijk P.M., 2003. Kinematic and structural development of the Çankırı Basin (Central Anatolia, Turkey). a paleostress inversion study. Tectonophysics, 364: 85-113.

Mamani M., Wörner G., and Sempere T., 2010. Geochemical variations in igneous rocks of the Central Andean orocline (13°S to 18°S): Tracing crustal thickening and magma generation through time and space. Geol. Soc. Am. Bull., 122: 162-182.

Marroni M., Frassi C., Göncüoğlu M.C., Di Vincenzo G., Pandolfi L., Rebay G., Ellero A. and Ottria G., 2014. Late Jurassic amphibolite facies metamorphism in the Intra-Pontide Suture Zone (Turkey): an eastward extension of the Vardar Ocean from the Balkans into Anatolia? J Geol. Soc. London, 171: 605-608.

McCulloch M.T. and Gamble J.A., 1991. Geochemical and geodynamical constraints on subduction zone magmatism. Earth Planet. Sci. Lett., 102: 358-374.

Okay A.I., 2000. Was the Late Triassic orogeny in Turkey caused by the collision of an oceanic plateau? In: E. Bozkurt, J.A. Winchester and J.A.D. Piper (Eds.), Tectonics and magmatism in Turkey and surrounding Area. Geol. Soc. London, Spec. Publ., 173: 25-41.

Okay A.I., Göncüoğlu M.C., 2004. The Karakaya complex: a review of data and concepts. Turk. J. Earth Sci., 13: 77: pt.

Okay A.I. and Tüysüz O., 1999. Tethyan sutures of northern Turkey. In: B. Durand, L. Jolivet, F. Horvath and M, Seranne (Eds.), The Mediterranean basins: Tertiary extension within the Alpine Orogen. Geol. Soc. London, Spec. Publ., 156: 475-515.

Okay A.I., Satır M., Maluski H., Siyako M., Monié P. Metzger R. and Akyuz S., 1996. Paleo- and Neo-Tethyan events in northwest Turkey: Geological and geochronological constraints. In: A. Yin, and M. Harrison (Eds.), Tectonics of Asia. Cambridge Univ. Press, p. 420-441.

Okay A.I., Sunal G., Sherlock S., Altıner D., Tüysüz O., Kylander-Clark A.R.C. and Aygül M., 2013. Early Cretaceous sedimentation and orogeny on the active margin of Eurasia: Southern Central Pontides, Turkey. Tectonics, 32: 1247-1271.

Okay A.I., Tüysüz O., Satır M., Özkan-Altıner S., Altıner D., Sherlock S. and Eren R.H., 2006. Cretaceous and Triassic subduction-accretion, HP/LT metamorphism and continental growth in the Central Pontides, Turkey. Geol. Soc. Am. Bull., 118: 1247-1269.

Özgen-Erdema N., Inan N., Akyazı M. and Tunog C., 2005. Benthonic foraminiferal assemblages and microfacies analysis of Paleocene–Eocene carbonate rocks in the Kastamonu region, Northern Turkey. J. Asian Earth Sci., 25: 403-417.

Pearce J.A., 1975. Basalt geochemistry used to investigate past tectonic environments on Cyprus. Tectonophysics, 25: 41-67.

Pearce J.A., 1983. The role of sub-continental lithosphere in magma genesis at active continental margins. In: C.J. Hawkesworth and M.J. Norry (Eds.), Continental basalts and mantle xenoliths. Nantwich (Shiva Publ.), p. 230-249.

Pearce J.A., 1996. A users guide to basalt discrimination diagrams. In: D.A. Wyman (Ed.), Trace Element geochemistry of volcanic rocks: Applications for massive sulphide exploration. Geol. Ass. Can., Short Course Notes, 12: 79-113.

Pearce J.A., 2008. Geochemical fingerprinting of oceanic basalts with applications to ophiolite classification and he search for Archean oceanic crust. Lithos, 100: 14-48.

Pearce J.A. and Peate D.W. 1995. Tectonic implications of the composition of volcanic arc magmas. Ann. Rev. Earth Planet. Sci., 23: 251-285.

Pearce J.A. and Stern R.J., 2006. Origin of back-arc basin magmas: Trace element and isotope perspectives. In: D. Christie (Ed.), Back-arc spreading Ssystems: Geological, biological, chemical and physical interactions, AGU Geophys. Monogr. Series, 166: 63-86.

Pearce J.A., Baker P.E., Harvey P.K. and Luff I.W. 1995. Geochemical evidence for subduction fluxes, mantle melting and fractional crystallization beneath the South Sandwich Island Arc. J. Petrol., 36: 1073-1109.

Peate D.W., Pearce J.A., Hawkesworth C.J., Colley H., Edwards C.M.H. and Hirose K. 1997. Geochemical variations in Vanuatu arc lavas: the role of subducted material and a variable mantle wedge composition. J. Petrol., 38: 1331-1358.

Peccerillo A. and Taylor S.R.,1976. Geochemistry of Eocene calc-alkaline volcanic rocks of the Kastamonu area, northern Turkey. Contrib. Mineral. Petrol., 58: 63-81.

Ramsay J.G., 1967. Folding and fracturing of rocks. McGraw-Hill, New York, 568 pp.

Rice S.P. and Robertson A.H.F. and Ustaömer T., 2006. Late Cretaceous-Early Cenozoic tectonic evolution of the Eurasian active margin in the Central and Eastern Pontides, northern Turkey. In: A.H.F. Robertson (Ed.), Tectonic development of the Eastern Mediterranean Region. Geol. Soc. London, Spec. Publ., 260: 413-445

Robertson A.H.F. and Ustaömer T., 2004. Tectonic evolution of the Intra-Pontide suture zone in the Armutlu Peninsula, NW Turkey. Tectonophysics, 381: 175-209.

Robertson A.H.F. and Ustaömer T., 2011. Role of tectonic-sedimentary mélange and Permian–Triassic cover units, central southern Turkey in Tethyan continental margin evolution. J. Asian Earth Sci., 40: 98-120

Robertson A.H.F., Clift P.D., Degnan P.J. and Jones G., 1991. Palaeogeographical and palaeotectonic evolution of the eastern Mediterranean Neotethys. Palaeogeogr. Palaeoclim. Palaeoecol., 87: 289-343.

Rojay B., 2013. Tectonic evolution of the Cretaceous Ankara ophiolitic mélange during the Late Cretaceous to pre-Miocene interval in Central Anatolia, Turkey. J. Geodyn., 65: 66-81.

Saccani E., 2015. A new method of discriminating different types of post-Archean ophiolitic basalts and their tectonic significance using Th-Nb and Ce-Dy-Yb systematics. Geosci. Front., 6 (1): 481-501.

Sayit K. and Göncüoğlu M.C., 2013. Geodynamic evolution of the Karakaya Mélange Complex, Turkey: a review of geological and petrological constraints. J Geodyn., 65: 56-65.

Sayit K., Marroni M., Göncüoğlu M.C., Pandolfi L., Ellero A., Ottria G. and Frassi C., 2015. Geological setting and geochemical signatures of the mafic rocks from the Intra-Pontide Suture Zone: implications for the geodynamic reconstruction of the Mesozoic Neotethys. Intern. J. Earth Sci., DOI 10.1007/s00531-015-1202-2, (in press).

Şengör A.M.C. and Yılmaz, Y., 1981. Tethyan evolution of Turkey: a plate tectonic approach. Tectonophysics, 75: 181-241.

Şengör A.M.C., Tüysüz O., Imren C., Sakinc M., Eyidogan H., Görür N., Le Pichon X. and Rangin C., 2005. The North Anatolian Fault: A new look. Ann. Rev. Earth Planet. Sci., 33: 37-112

Sissingh W., 1977. Biostratigraphy of Cretaceous calcareous nannoplancton. Geol. Mijnb., 56: 433-440.

Staudigel H., Plank T., White B. and Schmincke H-U., 1996. Geochemical fluxes during seafloor alteration of the basaltic upper oceanic crust: DSDP sites 417 and 418. AGU Geophys. Monogr., 96: 19-38.

Stern R.J., Kohut E., Bloomer S.H., Leybourne M., Fouch M. and Vervoort J., 2006. Subduction factory processes beneath the Guguan cross-chain, Mariana Arc: no role for sediments, are serpentinites important? Contrib. Mineral. Petrol., 151: 202-221.

Sun S.-S., and McDonough W. F., 1989. Chemical and isotopic systematics of oceanic basalts: implications for mantle composition and processes. In: A.D. Saunders and M.J. Norry (Eds.), Magmatism in the ocean basins. Geol. Soc. London Spec. Publ., 42: 313-345.

Tatsumi Y. and Kogiso T., 2003. The subduction factory: its role in the evolution of the Earth's crust and mantle. In: R.D. Larter and P.T. Leat (Eds.), Intra-oceanic subduction systems: Tectonic and magmatic processes. Geol. Soc. London Spec. Publ., 219: 55-80.

Tekin U.K., Göncüoğlu M.C., Pandolfi L. and Marroni M., 2012. Middle-Late Triassic radiolarian cherts from the Arkotdağ Mélange in northern Turkey: implications for the life span of the northern Neotethyan branch. Geodin. Acta, 25: 305-319.

Tüysüz O., Dellaloglu A.A. and Terzioglu N., 1995. A magmatic belt within the Neo-Tethyan suture zone and its role in the tectonic evolution of northern Turkey. Tectonophysics, 243: 173-191.

Winchester J.A. and Floyd P.A., 1977. Geochemical discrimination of different magma series and their differentiation products using immobile elements. Chem. Geol., 20: 25-343.

Yılmaz Y., 1990. Allochthonous terranes in the Tethyan Middle East, Anatolia and surrounding regions. Philos. Trans. Royal Soc. London, 331: 611-24.

Yılmaz Y., Genc S.C., Yiğitbaş E., Bozcu M. and Yılmaz K., 1995. Geological evolution of the late Mesozoic continental margin of Nortwestern Anatolia. Tectonophysics, 243: 155-171.

Yılmaz Y., Tüysüz O., Yiğitbaş E.C.Ş., Genç C.Ş. and Şengör A.M.C., 1997. Geology and tectonic evolution of the Pontides. In: A.G. Robinson (Ed.), Regional and petroleum geology of the Black Sea and surrounding region. Am. Ass. Petrol. Geol.s Mem., 68: 183-226.

Zindler A. and Hart S., 1986. Chemical geodynamics. Ann. Rev. Earth Planet. Sci., 14: 493-571.

Zuffa G.G., 1980. Hybrid arenites: their composition and classification. J. Sedim. Petr., 49: 21-29.

Received, September 16, 2015
Accepted, December 5, 2015